

Diagnostic Atlas of

RENAL PATHOLOGY



Enhanced
**DIGITAL
VERSION**
Included

4th Edition



Agnes B. Fogo
Michael Kashgarian

Any screen. Any time. Anywhere.

Activate the eBook version
of this title at no additional charge.



Elsevier eBooks for Practicing Clinicians gives you the power to browse and search content, view enhanced images, highlight and take notes—both online and offline.

Unlock your eBook today.

1. Visit expertconsult.inkling.com/redeem
2. Scratch box below to reveal your code
3. Type code into “Enter Code” box
4. Click “Redeem”
5. Log in or Sign up
6. Go to “My Library”

It's that easy!

Place Peel Off
Sticker Here

For technical assistance:
email expertconsult.help@elsevier.com
call 1-800-401-9962 (inside the US)
call +1-314-447-8300 (outside the US)

Use of the current edition of the electronic version of this book (eBook) is subject to the terms of the nontransferable, limited license granted on expertconsult.inkling.com. Access to the eBook is limited to the first individual who redeems the PIN, located on the inside cover of this book, at expertconsult.inkling.com and may not be transferred to another party by resale, lending, or other means.

Diagnostic Atlas of

RENAL PATHOLOGY

This page intentionally left blank

Diagnostic Atlas of RENAL PATHOLOGY

4th Edition

Agnes B. Fogo, MD

John L. Shapiro Professor of Pathology
Professor of Medicine and Pediatrics
Director, Renal/Electron Microscopy Laboratory
Department of Pathology, Microbiology and Immunology
Vanderbilt University Medical Center
Nashville, Tennessee

Michael Kashgarian, MD

Professor Emeritus of Pathology and Molecular, Cellular, and Developmental Biology
Department of Pathology
Yale University
New Haven, Connecticut



ELSEVIER

Elsevier
1600 John F. Kennedy Blvd.
Ste 1800
Philadelphia, PA 19103-2899

DIAGNOSTIC ATLAS OF RENAL PATHOLOGY, FOURTH EDITION

ISBN: 978-0-323-72163-9

Copyright © 2022 by Elsevier, Inc. All rights reserved.

No part of this publication may be reproduced or transmitted in any form or by any means, electronic or mechanical, including photocopying, recording, or any information storage and retrieval system, without permission in writing from the publisher. Details on how to seek permission, further information about the Publisher's permissions policies and our arrangements with organizations such as the Copyright Clearance Center and the Copyright Licensing Agency, can be found at our website: www.elsevier.com/permissions.

This book and the individual contributions contained in it are protected under copyright by the Publisher (other than as may be noted herein).

Notices

Knowledge and best practice in this field are constantly changing. As new research and experience broaden our understanding, changes in research methods, professional practices, or medical treatment may become necessary.

Practitioners and researchers must always rely on their own experience and knowledge in evaluating and using any information, methods, compounds or experiments described herein. Because of rapid advances in the medical sciences, in particular, independent verification of diagnoses and drug dosages should be made. To the fullest extent of the law, no responsibility is assumed by Elsevier, authors, editors or contributors for any injury and/or damage to persons or property as a matter of products liability, negligence or otherwise, or from any use or operation of any methods, products, instructions, or ideas contained in the material herein.

Library of Congress Control Number: 2021946977

Content Strategist: Nancy Duffy
Content Development Manager: Kathryn DeFrancesco
Content Development Specialist: Lisa Barnes
Publishing Services Manager: Deepthi Unni
Project Manager: Janish Ashwin Paul
Design Direction: Renee Duenow

Printed in India

Last digit is the print number: 9 8 7 6 5 4 3 2 1



Working together
to grow libraries in
developing countries

www.elsevier.com • www.bookaid.org

Preface

In the 5 years since the third edition of this Atlas, exciting advances have continued in the genetics, etiology, pathogenesis, and treatment of medical renal diseases. These advances have led to a therapeutic focus on a more specific and personalized approach and, in turn, further emphasized the importance and central role of the renal biopsy in patient management. We are therefore excited to present the fourth edition of this renal pathology textbook. The organization of this edition follows that of the previous editions, with each of the sections being expanded and updated. New insights into a spectrum of kidney diseases, including C3 glomerulopathies, fibrillary glomerulonephritis, membranous nephropathy, and IgA nephropathy, have been added. New sections on IgA-dominant infection-related glomerulonephritis and collagen III glomerulopathy have been added. Updated classifications of various lesions, including transplant, autosomal tubulointerstitial diseases, cystic diseases, and neoplasms, have been included. Sections on genetics, etiology, and pathogenesis have also been expanded. References have been updated and continue to be focused, rather than encyclopedic, with emphasis on classic and most recent literature on each subject.

Because this is primarily an atlas, we have also added numerous new images. These include illustrations of additional entities and expanded illustrations of the spectrum of lesions present in diseases already included in the previous edition and updated differential diagnosis and key diagnostic features tables for each section. In addition, we have added new elements, including many color-coded electron microscopic images within the printed version and animated schemas of evolution of selected glomerular lesions in the online version. Together with the numerous images and focused text, this atlas thus provides in-depth and detailed illustrations of a large spectrum of morphologic lesions encountered in the renal biopsy and an approach to differential diagnosis and key prognostic, pathogenetic, and etiologic information.

Agnes B. Fogo
Michael Kashgarian

This page intentionally left blank

Acknowledgments

Renal pathology is an exciting process of integrating complex information, relying on a team of nephrologists, pathologists, and highly skilled laboratory personnel. Similar teamwork has gone into the preparation of this book. The ongoing dedication and partnership with Dr. Michael Kashgarian have been essential to the success and joy of our project. I would also like to thank my renal pathology laboratory team—my past fellows and colleagues—who have been essential for this work. I continue to be grateful to my past fellows, especially Drs. Paisit Paueksakon, Xochi Geiger, Patricia Revelo, Michele Rossini, Aruna Dash, Huma Fatima, Paul Persad, Meghan Kapp, and Mark Lusco, who have searched and hunted for the most instructive and beautiful examples of lesions to expand this Atlas. I am also indebted to the expert help of the late Brent Weedman for imaging and photography assistance for previous editions, and to Dominic Doyle with his masterful job translating my drawings into beautiful schemas and animations.

Lastly, I would like to thank my husband, Byron, and my children, Katherine, Michelle, and Kristin, for their enthusiastic support and encouragement for all of my endeavors, and my grandchildren, Mila, Miles, Ethan, Blake and Brooklyn, who bring joy to our family in all that we do.

Agnes B. Fogo

This page intentionally left blank

Contents

CHAPTER 1

Approach to Diagnosis of the Kidney Biopsy, 1

CHAPTER 2

Normal Growth and Maturation, 7

CHAPTER 3

Glomerular Diseases, 15

PRIMARY GLOMERULAR DISEASES, 16

Glomerular Diseases That Cause Nephrotic Syndrome:

Nonimmune Complex, 16

Minimal Change Disease and Focal Segmental Glomerulosclerosis: Introduction, 16

Minimal Change Disease, 17

Focal Segmental Glomerulosclerosis, 20

Collapsing Glomerulopathy, 34

Tip Lesion Variant of Focal Segmental Glomerulosclerosis, 40

Cellular Variant of Focal Segmental Glomerulosclerosis, 42

Perihilar Variant of Focal Segmental Glomerulosclerosis, 44

Congenital Nephrotic Syndrome of Finnish Type, 46

Diffuse Mesangial Sclerosis, 49

Frasier Syndrome, 52

Glomerular Diseases That Cause Nephrotic/Nephritic Syndrome: Complement-Related, 54

C1Q Nephropathy, 54

C3 Glomerulopathies, 56

Dense Deposit Disease, 57

C3 Glomerulonephritis, 64

Glomerular Diseases That Cause Nephrotic Syndrome Because of Deposits, 69

Membranous Nephropathy, 69

Membranoproliferative Glomerulonephritis, 85

Fibrillary Glomerulonephritis, 99

Immunotactoid Glomerulopathy, 107

Glomerular Diseases That Cause Hematuria or Nephritic Syndrome: Immune Complex, 111

Acute Postinfectious Glomerulonephritis, 111

Immunoglobulin A–Dominant Infection-Related Glomerulonephritis, 122

Immunoglobulin A Nephropathy, 127

SECONDARY GLOMERULAR DISEASES, 140**Diseases Associated With Nephrotic Syndrome, 140**

- Monoclonal Immunoglobulin Deposition Disease, 140
- Amyloidosis, 155
- Proliferative Glomerulonephritis with Monoclonal Deposits, 165
- HIV-Associated Nephropathy, 169
- Sickle Cell Nephropathy, 175
- Fabry Disease, 182
- Lipoprotein Glomerulopathy, 187
- Lecithin-Cholesterol Acyltransferase Deficiency, 189
- Hereditary Focal Segmental Glomerulosclerosis, 193

Diseases Associated With Nephritic Syndrome or Rapidly Progressive Glomerulonephritis: Immune-Mediated, 195

- Lupus Nephritis, 195
- Atypical Presentations of Renal Involvement in Systemic Lupus Erythematosus, 212
- Immunoglobulin A Vasculitis (Henoch–Schönlein Purpura), 224
- Mixed Connective Tissue Disease, 233
- Mixed Cryoglobulinemia, 239
- Anti-Glomerular Basement Membrane Antibody–Mediated Glomerulonephritis, 251

Diseases Associated With the Nephritic Syndrome or Rapidly Progressive Glomerulonephritis: Pauci-Immune- or Nonimmune-Mediated, 259

- Antineutrophil Cytoplasmic Autoantibody–Associated Small-Vessel Vasculitis (Pauci-Immune Glomerulonephritis), 259
- Microscopic Polyangiitis, 261
- Granulomatosis with Polyangiitis (Wegener’s Granulomatosis), 263
- Eosinophilic Granulomatosis with Polyangiitis (Churg–Strauss Syndrome), 272
- Polyarteritis Nodosa, 272

Diseases With Abnormal Collagen/Basement Membranes, 273

- Alport Syndrome, 273
- Thin Basement Membrane Lesions, 283
- Nail-Patella Syndrome, 286
- Type III Collagen Glomerulopathy, 288

Glomerular Involvement With Bacterial Infections, 291

- Subacute Bacterial Endocarditis, 291
- Shunt Nephritis, 297

CHAPTER 4**Vascular Diseases, 305****Diabetic Nephropathy, 305**

- Etiology/Pathogenesis, 315

Thrombotic Microangiopathy/Thrombotic Thrombocytopenic Purpura, 318

- Etiology/Pathogenesis, 328

Scleroderma (Systemic Sclerosis), 333

- Etiology/Pathogenesis, 334

Antiphospholipid Antibody Disease, 340

- Etiology/Pathogenesis, 341

Preeclampsia and Eclampsia, 341

- Pathology, 341
- Etiology/Pathogenesis, 348

- Fibromuscular Dysplasia, 349**
 - Etiology/Pathogenesis, 351
 - Pathology, 351
- Arterionephrosclerosis, 354**
 - Etiology/Pathogenesis, 364
- Accelerated/Severe Hypertension, 366**
 - Etiology/Pathogenesis, 368
- Atheroemboli, 371**
 - Etiology/Pathogenesis, 375

CHAPTER 5

Tubulointerstitial Diseases, 377

- Introduction, 378**
- Infections of the Kidney, 379**
- Acute Pyelonephritis, 379**
 - Etiology/Pathogenesis, 382
 - Key Diagnostic Feature of Acute Pyelonephritis, 384
 - Differential Diagnosis of Acute Pyelonephritis, 384
- Chronic Pyelonephritis and Reflux Nephropathy, 385**
 - Etiology/Pathogenesis, 388
 - Key Diagnostic Features of Chronic Pyelonephritis/Reflux Nephropathy, 388
 - Differential Diagnosis of Chronic Pyelonephritis/Reflux Nephropathy, 388
- Xanthogranulomatous Pyelonephritis, 388**
 - Etiology/Pathogenesis, 388
- Malakoplakia, 388**
 - Etiology/Pathogenesis, 391
- Acute Tubulointerstitial Nephritis—Viral Infection, 391**
 - Etiology/Pathogenesis, 392
- Acute Tubulointerstitial Nephritis—Drug-Related, 392**
 - Etiology/Pathogenesis, 392
- Tubulointerstitial Nephritis With Uveitis, 399**
- Anti-Tubular Basement Membrane Antibody Nephritis, 400**
 - Etiology/Pathogenesis, 400
 - Key Diagnostic Features of Anti-TBM Antibody Nephritis, 402
 - Differential Diagnosis of Anti-TBM Antibody Nephritis, 402
- Idiopathic Hypocomplementemic Tubulointerstitial Nephritis, 403**
- IgG4-Related Tubulointerstitial Nephritis, 403**
 - Etiology/Pathogenesis, 403
 - Key Diagnostic Features of IgG4-Related Tubulointerstitial Nephritis, 408
 - Differential Diagnosis of IgG4-Related Tubulointerstitial Nephritis, 408
- Interstitial Nephritis of Sjögren Syndrome, 409**
- Sarcoidosis, 409**
 - Etiology/Pathogenesis, 413
 - Key Diagnostic Feature of Sarcoidosis, 413
 - Differential Diagnosis of Sarcoidosis, 413
- Acute Kidney Injury/Acute Tubular Injury, 414**
 - Ischemic Acute Tubular Injury, 415
 - Acute Phosphate Nephropathy, 421
 - Nephrotoxic Acute Tubular Necrosis, 426

- Warfarin-Induced Acute Kidney Injury/Anticoagulant-Related Nephropathy, 435**
- Heavy Metal Nephropathy (Lead and Cadmium Nephropathy), 435**
 - Etiology/Pathogenesis, 436
- Analgesic Nephropathy and Papillary Necrosis, 437**
 - Etiology/Pathogenesis, 440
 - Key Diagnostic Feature of Chronic Tubulointerstitial Nephritis, 440
- Monoclonal Gammopathy of Renal Significance, 440**
- Light Chain Cast Nephropathy and Tubulopathy, 440**
 - Etiology/Pathogenesis, 448
 - Key Diagnostic Features of Light Chain Cast Nephropathy, 450
 - Key Diagnostic Features of Light Chain Proximal Tubulopathy, 450
- Tubular Crystallopathies, 451**
 - Cystinosis, 451
 - Nephrocalcinosis, 455
 - Oxalosis, 456
 - Urate Nephropathy, 461
- Drug-Induced Crystallopathies, 462**
 - Etiology/Pathogenesis, 463
- Lithium Nephropathy, 464**
 - Key Diagnostic Findings of Lithium Nephropathy, 464
- Aristolochic Acid Nephropathy, 464**

CHAPTER 6

Endemic Nephropathies, 465

- Introduction, 465
- Aristolochic Acid Nephropathy (Chinese Herb Nephropathy, Balkan Endemic Nephropathy), 465**
- Other Endemic Fibrosing Nephropathies, 467**
 - Ochratoxin Nephropathy, 467
 - Chronic Interstitial Nephritis in Agricultural Communities in Sri Lanka, 467
 - Chronic Interstitial Nephritis in Agricultural Communities—Mesoamerican Nephropathy, 467
 - Apolipoprotein L1-Associated Nephropathies, 469

CHAPTER 7

Chronic Kidney Disease, 471

- Introduction, 471
- Age-Related Sclerosis, 472
- Glomerular Versus Tubulointerstitial Versus Vascular Disease, 475
- Segmental Glomerulosclerosis: Primary Versus Secondary, 475

CHAPTER 8

Renal Transplantation, 477

- Introduction, 477
- Evaluation of Donor Kidneys, 481
- Classification of Rejection, 482
 - Etiology/Pathogenesis, 482

Antibody-Mediated Rejection, 482

Key Diagnostic Features of Antibody-Mediated Rejection, 485

Chronic Active Antibody-Mediated Rejection and Transplant Glomerulopathy, 485

Key Diagnostic Feature of Chronic Active Antibody-Mediated Rejection and Transplant Glomerulopathy, 486

Acute T Cell-Mediated Rejection, 486

Grade I Acute T Cell-Mediated Rejection, 487

Grade II Acute T Cell-Mediated Rejection, 489

Grade III Acute T Cell-Mediated Rejection, 489

Chronic Active T Cell-Mediated Rejection, 492**Interstitial Fibrosis/Tubular Atrophy, 492****Molecular Profiling of Rejection, 494****Calcineurin Inhibitor Nephrotoxicity, 494**

Etiology/Pathogenesis, 494

Key Diagnostic Features of Calcineurin Inhibitor Nephrotoxicity, 494

mTOR Inhibitor Toxicity, 494**De Novo and Recurrent Thrombotic Microangiopathy in Allografts, 497****Posttransplant Lymphoproliferative Disease, 497**

Etiology/Pathogenesis, 498

Differential Diagnosis of Posttransplant Lymphoproliferative Disease, 498

Viral Infections, 499

Key Diagnostic Features of Polyoma Virus Nephropathy, 504

Recurrent Renal Disease, 505**CHAPTER 9****Cystic Diseases of the Kidney, 507****Introduction, 507****Autosomal Dominant Polycystic Kidney Disease, 507**

Pathology, 508

Etiology/Pathogenesis, 513

Autosomal Recessive Polycystic Kidney Disease, 513

Pathology, 513

Etiology/Pathogenesis, 513

Nephronophthisis, 515**Autosomal Dominant Tubulointerstitial Kidney Disease, 516****Medullary Sponge Kidney, 519****Acquired Cystic Disease, 520****Cystic Renal Dysplasia, 521**

Etiology/Pathogenesis, 521

CHAPTER 10**Renal Neoplasia, 525****Introduction, 525****Renal Neoplasms, 527**

Benign Epithelial Neoplasms, 527

Renal Cell Carcinomas, 527

Nephroblastoma (Wilms Tumor), 540

Etiology/Pathogenesis, 540

Renal Angiomyolipoma, 543

Urothelial (Transitional Cell) Carcinoma of the Renal Pelvis, 544

Etiology/Pathogenesis, 545

Index, 547

Approach to Diagnosis of the Kidney Biopsy

The approach to diagnosing disease in renal biopsy specimens requires information from several different sources to be integrated into a single interpretation. The sources include the clinical data and examination by light microscopy, immunohistology, and electron microscopy. Each of the sources has several individual variables that must be either included or dismissed in the final evaluation. George Boole in his books *The Mathematical Analysis of Logic* (1847) and *An Investigation of the Laws of Thought* (1854) introduced a branch of algebra in which the values of the variables are the truth values *true* and *false*, which are usually denoted as 1 and 0, respectively, and form the basis of our current digital world. This expanded the range of applications that can be handled from propositions that have only two potential values to those that have many. Thus, in many ways, the complex analysis of how renal biopsy findings lead to a diagnosis can be viewed as an exercise in Boolean logic. With increasing utilization of digital pathology, applications of machine learning and artificial intelligence in biopsy diagnosis are beginning to be used as an *adjunct* to diagnosis, prognosis, and therapy. Computer algorithms use Bayesian decision theory to unify results from light, immunofluorescence, and electron microscopy data with molecular data and clinical presentation. Bayes' theorem determines the likelihood of a result occurring, based on previous outcomes.

Because Bayesian statistical methods start out with existing data and beliefs, high or multilevel problem solving still depends on utilization and semiquantification of what the pathologist sees in the biopsy. Bayes' theorem provides a way to revise existing predictions or theories given new or additional evidence. Thus the addition of immunofluorescence microscopy and then electron microscopy to light microscopy and then the molecular profile and then the clinical presentation, sequentially one layer after another, increases the conditional probability of the diagnosis. When all the data of a single biopsy are analyzed further using artificial intelligence algorithms in the background of an existing data set, the predictive value of that biopsy in selection of therapy and outcome is greatly enhanced. Future artificial intelligence advances may add subvisual findings linked to disease outcomes that can be mined to discern previously unknown molecular mechanisms of disease. In this book, we will use the traditional microscopy tools and approaches to illustrate how a differential diagnosis is reached and to show the key features distinguishing various entities with overlapping features.

In addition to the diagnosis, the stage of disease and primary site of injury should be determined. From the clinical and laboratory data, a decision must be made whether the disease process is acute or chronic and whether it is tubular disease, interstitial disease, vascular disease, glomerular disease, or a combination of any of these. If there are glomerular lesions, we must determine if they are hypercellular/proliferative, necrotizing, or sclerosing. Subsequently, if there is no hypercellularity/proliferation, we must determine by immunofluorescence whether immunoglobulins and/or complement deposits are present or not. If no immunoglobulins or complement deposits are seen, we must determine by electron microscopy whether podocytes are extensively effaced or not. At each step we make a true or false decision and form a lattice (i.e., *algorithm* or *schema*, [Figs. 1.1–1.4](#)) to narrow our diagnostic choices. Alternatively, sets of decisions are made with the variables of each of the biopsy sources of information (i.e., light microscopy, immunohistology, and electron microscopy) forming separate overlapping Boolean logic circles ([Figs. 1.5 and 1.6](#)). Finally, each of the lattices or circles can be superimposed and their intersections used to arrive at a final interpretation or diagnosis.

For glomerular diseases, the pattern of injury by light microscopy should be specified ([Table 1.1](#)), such as into mesangial versus endocapillary hypercellularity, or necrosis, crescents, or sclerosis, noting that mixed patterns of glomerular injury often coexist. If immunoglobulins are present, the localization and pattern of deposition, such as the peripheral capillary, mesangial, or both ([Table 1.2](#)), should

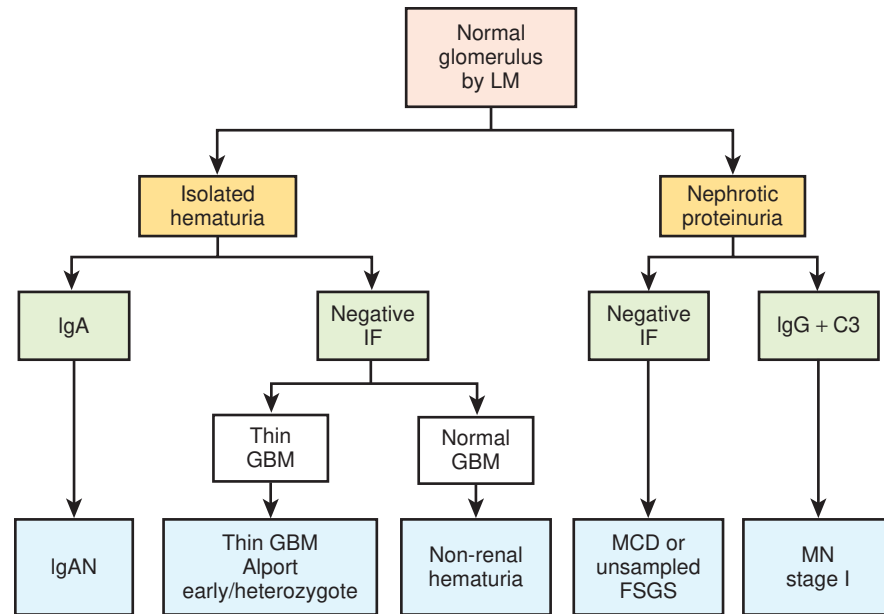


FIG. 1.1 Algorithmic approach when glomeruli appear normal by light microscopy (LM). Depending on the clinical setting, whether isolated hematuria or with nephrotic proteinuria, and whether immune deposits are present or not by immunofluorescence (IF, green boxes), varying diseases are included in the differential. These possibilities are then assessed further by electron microscopy. *FSGS*, Focal segmental glomerulosclerosis; *GBM*, glomerular basement membranes; *IgAN*, immunoglobulin A nephropathy; *MCD*, minimal change disease; *MN*, membranous nephropathy.

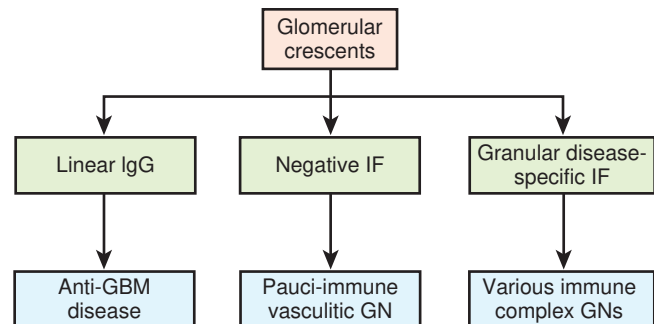


FIG. 1.2 Algorithmic approach when glomeruli show crescents by light microscopy. Depending on whether immune staining is present or not by immunofluorescence (IF, green boxes) and whether it is linear along glomerular basement membranes (GBM) or granular, varying diseases are included in the differential. *GN*, Glomerulonephritis.

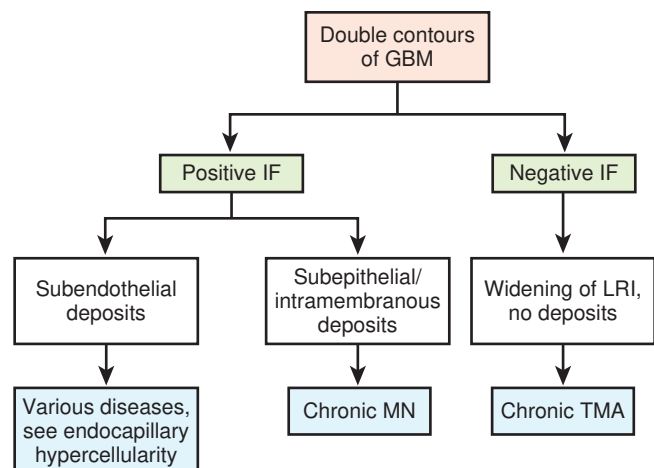


FIG. 1.3 Algorithmic approach when glomeruli show double contours of the glomerular basement membranes (GBM) by light microscopy. Depending on whether immune deposits are present or not by immunofluorescence (IF, green boxes), and depending on the specific location of deposits by electron microscopy, immune complex diseases or chronic endothelial injury (chronic thrombotic microangiopathy, TMA) are diagnosed. *LRI*, Lamina rara interna; *MN*, membranous nephropathy.

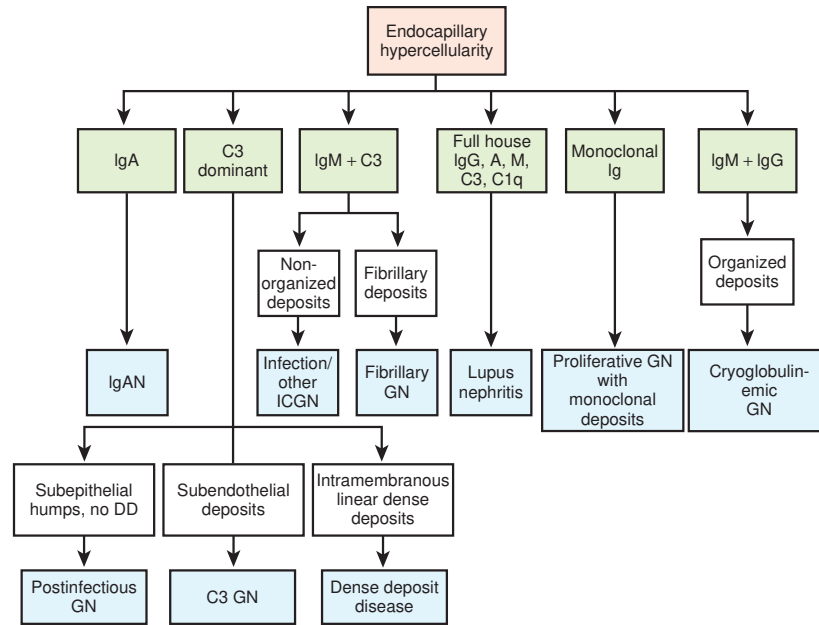


FIG. 1.4 Algorithmic approach when glomeruli show endocapillary proliferation/hypercellularity by light microscopy. Depending on the type and possible clonality of deposits by immunofluorescence (IF, green boxes), varying diseases are included in the differential. Electron microscopy differentiates organized versus nonorganized deposits. In the case of C3-dominant deposits, electron microscopic findings contribute to the final diagnosis. *DD*, Dense deposits; *GN*, glomerulonephritis; *ICGN*, immune complex glomerulonephritis.



FIG. 1.5 Boolean circle analysis of glomerular lesions with immunoglobulin A (IgA). The contribution of information from each of the techniques (i.e., light microscopy, immunofluorescence microscopy, and electron microscopy) overlaps to give the differential diagnosis by adding additional variables. *HS purpura*, Henoch–Schönlein purpura (also known as *IgA vasculitis*).

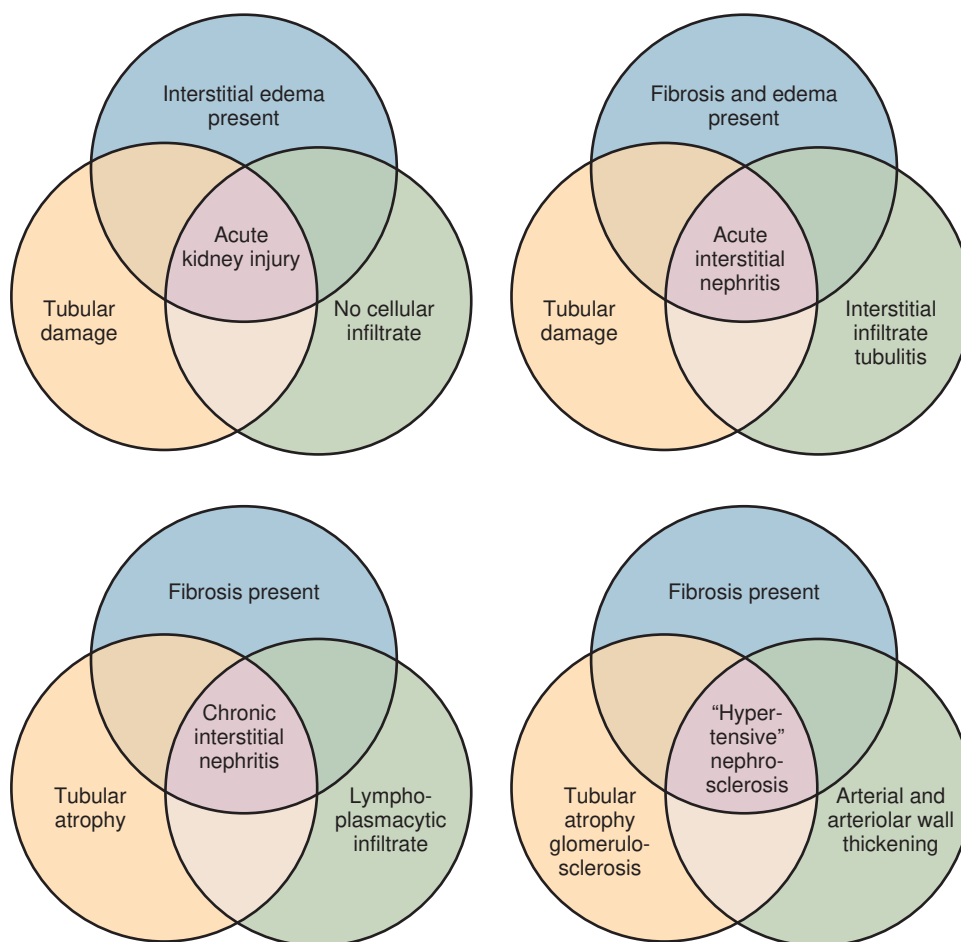


FIG. 1.6 Boolean circle analysis of tubular interstitial lesions. The contribution of information from different microscopic parameters (i.e., interstitial edema or fibrosis, epithelial integrity, presence or absence of interstitial infiltrate, and vascular integrity) overlaps to give the differential diagnosis by adding or deleting each of the possible variables.

TABLE 1.1 Light Microscopic Findings

Glomerular findings

Distributional descriptors

Focal	Involving less than 50% of glomeruli
Diffuse	Involving 50% or more of glomeruli
Segmental	Involving part of a glomerular tuft
Global	Involving all of a glomerular tuft
Lobular (hypersegmented)	Appearance because of endocapillary hypercellularity and consolidation of segments
Nodular	Relatively acellular, round areas of mesangial matrix expansion
Membranoproliferative	Combined capillary wall thickening with double contours of GBM and mesangial and/or endocapillary hypercellularity
Mesangium	Stalk region of capillary loop with mesangial cells surrounded by matrix

Lesional descriptors

Membranous thickening	Global thickening of peripheral capillary walls with spikes
Wire loop	Thick, rigid appearance of capillary loop because of massive subendothelial deposits

TABLE 1.1 Light Microscopic Findings—cont'd**Glomerular findings**

Tram-track	Double contour of glomerular basement membrane because of deposits and/or circumferential cellular interposition
Mesangial hypercellularity	Four or more nuclei in a peripheral mesangial segment
Endocapillary hypercellularity	Increased cellularity internal to the GBM composed of leukocytes, endothelial cells, and/or mesangial cells
Extracapillary hypercellularity (crescents)	Increased cellularity in Bowman's space
Sclerosis (focal and/or segmental)	Increased extracellular matrix expanding the mesangium and obliterating capillary lumens
Necrosis	Destruction of cells and matrix with deposition of fibrinoid material
Mesangiolysis	Loss of mesangial architecture with lysis of mesangial matrix and loss of mesangial cells
Hyaline	Glassy eosinophilic extracellular material

GBM, Glomerular basement membrane.

TABLE 1.2 Immunofluorescence Findings

Distributional descriptors for immune proteins, complement components, and fibrinogen (IgG, IgA, IgM, kappa, lambda, C3, C1q, C4d, fibrinogen) (specify if focal/diffuse, global/segmental):
Diffuse vs. focal peripheral capillary wall
Global vs. segmental peripheral capillary wall
Mesangial
Peritubular
Interstitial (peritubular) capillary
Fluorescent patterns
Linear
Finely granular
Coarsely granular

Ig, Immunoglobulin.

be noted. On ultrastructural examination, changes should be noted in each of the cell types, such as the podocytes, endothelial cells, and mesangial cells, as well as the basement membranes, mesangial matrix, and tubulointerstitium (Table 1.3). The final diagnosis is made based on the presence or absence of a convergence of all of these findings.

If the process predominantly involves the tubulointerstitium (Table 1.4), we must determine whether the process is acute or chronic. A disproportionate increase in interstitial inflammatory cells indicates a tubulointerstitial nephritis, with edema in acute interstitial nephritis and fibrosis and atrophy of tubules in chronic interstitial nephritis. Possible specific underlying etiologies are then assessed; for example, we can assess for monoclonal light chain casts, viral inclusions, or evidence of deposits.

Arteriosclerosis with intimal and medial thickening of arteries is typical in any chronic kidney disease, but vascular lesions may also be the primary abnormality underlying renal dysfunction. Thrombosis, necrosis, vasculitis, and cholesterol emboli are examples of specific vascular lesions associated with specific diagnoses (Table 1.5).

Systematic assessment of each of these anatomic compartments, and integration of each modality of tissue examination with the clinical history, then allows a specific diagnosis to be made. Ideally, a disease entity/pathogenic type (if the disease entity is not known) is diagnosed. Lastly, specific scoring/grading/classification may be applied to arrive at a complete clinicopathologic diagnosis, driven by a logical pathogenic/etiologic approach.

TABLE 1.3 Electron Microscopic Findings

Capillary loops	Patent, collapsed, mesangial/cellular interposition, thrombosed
Basement membranes	Normal, thickened, attenuated, laminated, basket/weaving, duplicated
Podocytes	Focal, segmental, or global effacement, sclerotic
Endothelial cells	Fenestrations preserved, swollen, reticular aggregates (tubuloreticular arrays) Endothelialitis, luminal leukocytes
Mesangial cells	Mild or marked increase, lysis
Mesangial matrix	Mild or marked increase, nodular, Kimmelstiel–Wilson nodules
Electron-opaque deposits	Dense, organized, granular, fibrillar, “finger print” Subepithelial and/or intramembranous, “humps” Subendothelial (occasional, numerous, paramesangial) Mesangial (occasional, abundant)
Tubules	Swollen, vacuolated, apical blebbing, apoptotic, necrosis, mitochondrial changes, epithelial detachment, deposits along the TBM (powdery or dense), viral inclusions, crystals
Interstitialium	Increased collagen, leukocytes, peritubular capillary multilaminated basement membranes, crystals

TBM, Tubular basement membranes.

TABLE 1.4 Tubulointerstitial Findings

Fibrosis	Focal, diffuse, striped, percentage of sample involved
Edema	Focal, diffuse
Interstitial infiltrate	Neutrophils, eosinophils, lymphocytes, plasma cells, macrophages
Tubules	Dilated lumens, cell swelling, apical blebbing, vacuolization, flattening, cell detachment, mitosis, hyaline droplets, tubular debris, atrophy, casts

TABLE 1.5 Vascular Findings

Arteries	Medial thickening, medial necrosis, mucinous degeneration, intimal proliferation, neutrophil infiltration, atheroemboli, elastin duplication
Arterioles	Intimal and medial hyalinosis, medial hyperplasia, fibrinoid necrosis, thrombosis, endothelialitis

We will elucidate the specific lesions characteristic of a range of common kidney diseases, discussed in the context of the primary anatomic site of injury, which may be the glomerular, vascular, or tubulointerstitial compartment. The glomerular diseases are best approached as either primary or those secondary to systemic disease and by integrating with common clinical presentation, such as nephrotic versus nephritic syndrome versus rapidly progressive glomerulonephritis. We will also discuss lesions in the transplant kidney and cystic and neoplastic diseases.

Selected Reading

- Haas M, Seshan SV, Barisoni L, et al. Consensus definitions for glomerular lesions by light and electron microscopy: Recommendations from a work. *Kidney Int.* 2020;98:1120-1134.
- Loupy A, Aubert O, Orandi BJ, et al. Prediction system for risk of allograft loss in patients receiving kidney transplants: international derivation and validation study. *Br Med J.* 2019;366:l4923.
- Sethi S, Haas M, Markowitz GS, et al. Mayo Clinic/Renal Pathology Society consensus report on pathologic classification, diagnosis, and reporting of GN. *J Am Soc Nephrol.* 2016;27:1278-1287.

Normal Growth and Maturation

The normal glomerulus consists of a complex branching network of capillaries originating at the afferent arteriole and draining into the efferent arteriole (Figs. 2.1–2.3). The glomerulus contains three resident cell types: mesangial, endothelial, and epithelial. The visceral epithelial cells (also called *podocytes*) cover the urinary surface of the glomerular basement membrane (GBM) with foot processes, with intervening slit diaphragms. Endothelial cells are opposed to the inner surface of the GBM and are fenestrated (Figs. 2.4 and 2.5). At the stalk of the capillary, the endothelial cell is separated from the mesangial cells by the intervening mesangial matrix. The term *endocapillary* is used to describe hypercellularity/proliferation filling up the capillary lumen, contributed to by increased mesangial, endothelial, and infiltrating inflammatory cells. In contrast, *extracapillary proliferation* refers to proliferation of the parietal epithelial cells that line Bowman's capsule. Specific lesions are described according to their distribution as being segmental versus global or diffuse versus focal. Specialized terminology is also used to describe the specific lesions. A list of commonly used terms and their definitions is provided in Table 2.1.

The mesangial cell is a contractile cell that lies embedded in the mesangial matrix in the stalk region of the capillary loops and is attached to anchor sites at the ends of the loop by thin extensions of

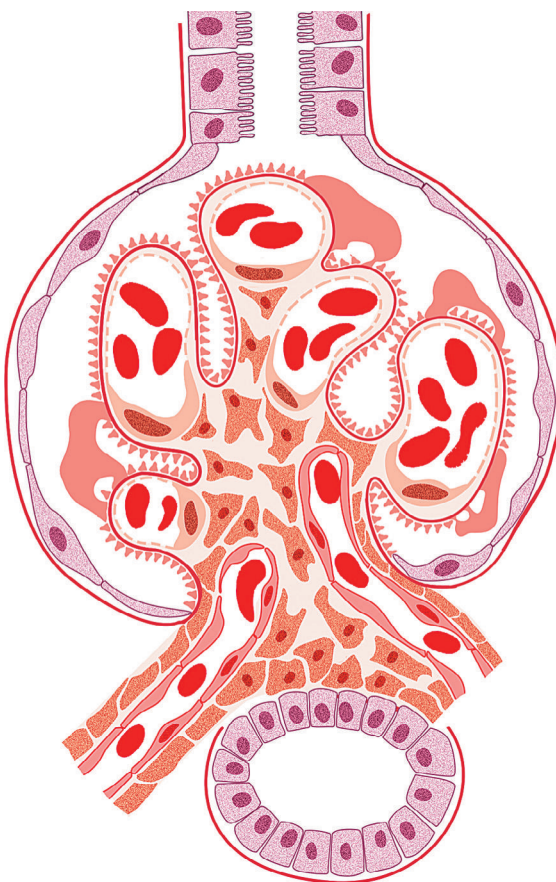


FIG. 2.1 In the normal glomerulus, the capillary loops are open, the mesangial areas have no more than three nuclei each, and foot processes are intact, without any deposits or proliferation.

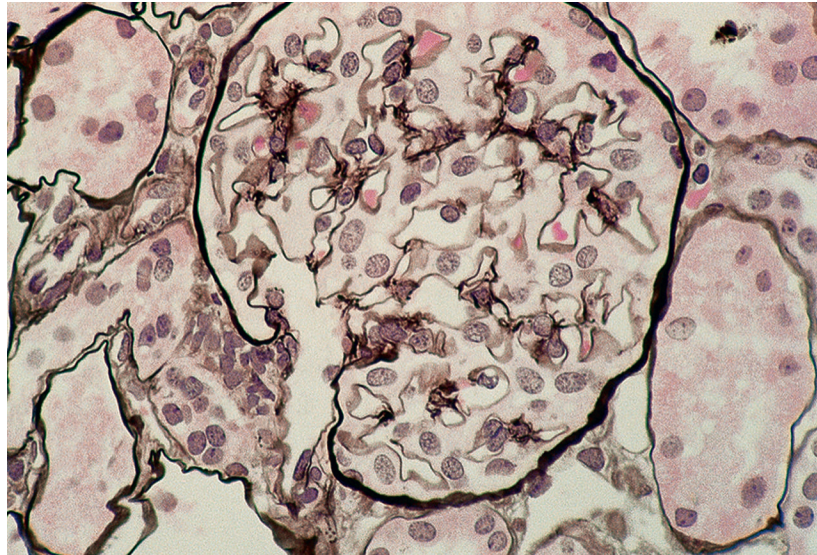


FIG. 2.2 The normal glomerulus has thin, delicate glomerular basement membranes, three or fewer mesangial cell nuclei per mesangial area, and is surrounded by Bowman's capsule. The adjacent tubules show a thin, delicate tubular basement membrane without lamellation or surrounding interstitial fibrosis. The vascular pole shows surrounding extraglomerular mesangial cells. The apparent mesangial cellularity of the glomerulus is highly dependent on the thickness of the section, and it is recommended that renal biopsies be cut at 2 μm thickness. This plastic embedded section is cut at 1 μm (Jones silver stain, $\times 400$).

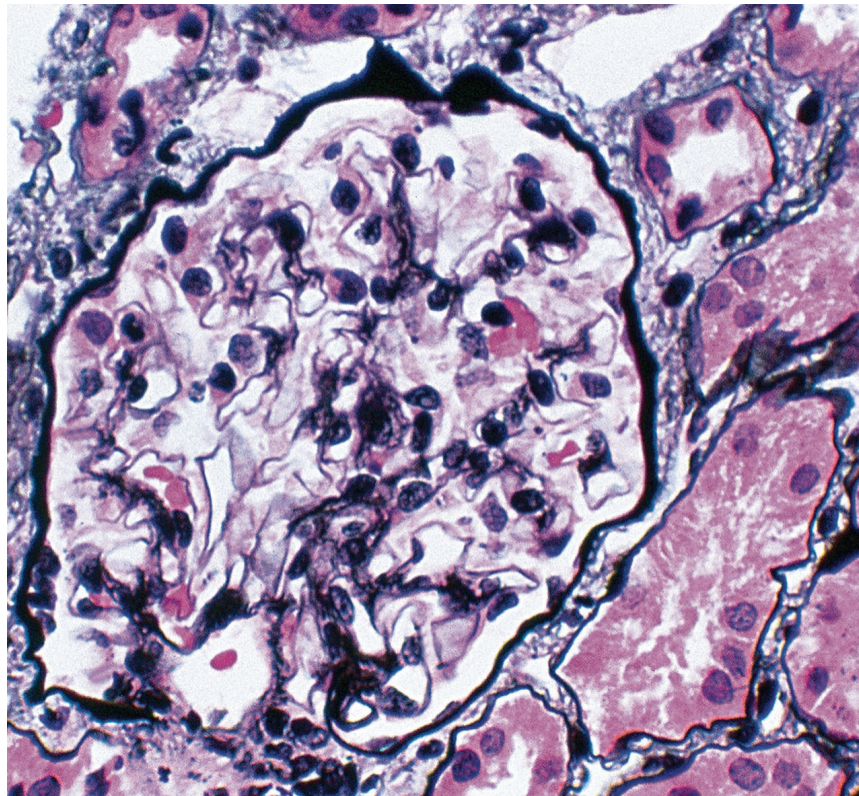


FIG. 2.3 This paraffin-embedded 2- μm section illustrates a normal glomerulus with normal vascular pole with minimal periglomerular interstitial fibrosis and surrounding intact tubules. Mesangial cellularity and matrix are within normal limits (Jones silver stain, $\times 400$).

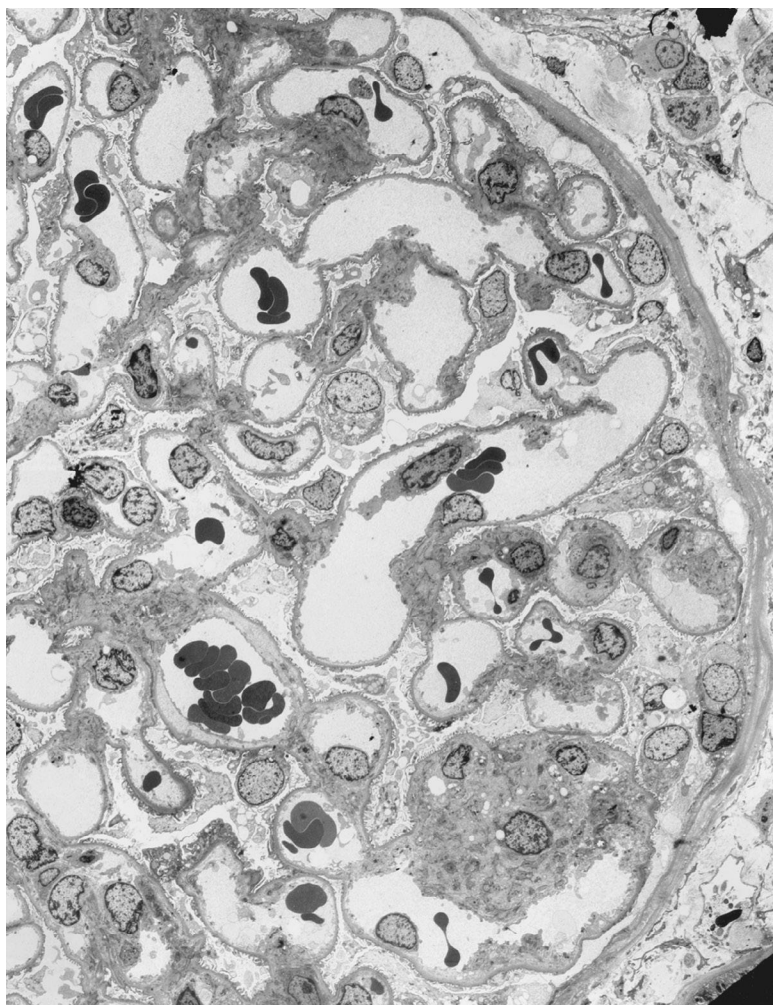


FIG. 2.4 The normal glomerular basement membrane in the adult is approximately 325 to 375 nm in thickness. Overlying podocytes show intact foot processes with minimal effacement in this case. The mesangial matrix surrounds mesangial cells without expansion or hypercellularity. Endothelial cells show normal fenestration. The parietal cells lining Bowman's capsule are flat and squamous in appearance (transmission electron microscopy, $\times 1500$).

its cytoplasm. Normally, up to three mesangial cell nuclei are present per mesangial area. The hilar area of the tuft normally can contain increased mesangial cells. The GBM consists of three layers distinguished by electron microscopy, the central broadest lamina densa and the less electron-dense zones of lamina rara externa and interna (see [Figs. 2.4](#) and [2.5](#)).

The glomerulus is surrounded by Bowman's capsule, which is lined by parietal epithelial cells. These are continuous with the proximal tubule, identifiable by its periodic acid Schiff (PAS)-positive brush border. The efferent and afferent arterioles can be distinguished morphologically in favorably oriented sections or by tracing their origins on serial sections. Segmental, interlobular, and arcuate arteries may also be present in the renal biopsy specimen. The cortical biopsy also allows for the assessment of the tubules and interstitium. Proximal tubules are readily identified by their PAS-positive brush border, lacking in the distal tubules. Collecting ducts show cuboidal, cobblestone-like epithelium. The medulla, and even the urothelium of the calyx, may also be included in the biopsy.

During fetal maturation, the glomerular capillary tufts have a simple branching pattern with small capillary lumina and are covered by large, cuboidal, darkly staining epithelial cells ([Figs. 2.6–2.8](#)). The cells lining Bowman's space undergo change from initial tall columnar to cuboidal to flattened epithelial cells, except for those located at the opening of the proximal tubule, where cells remain taller. Intermediate

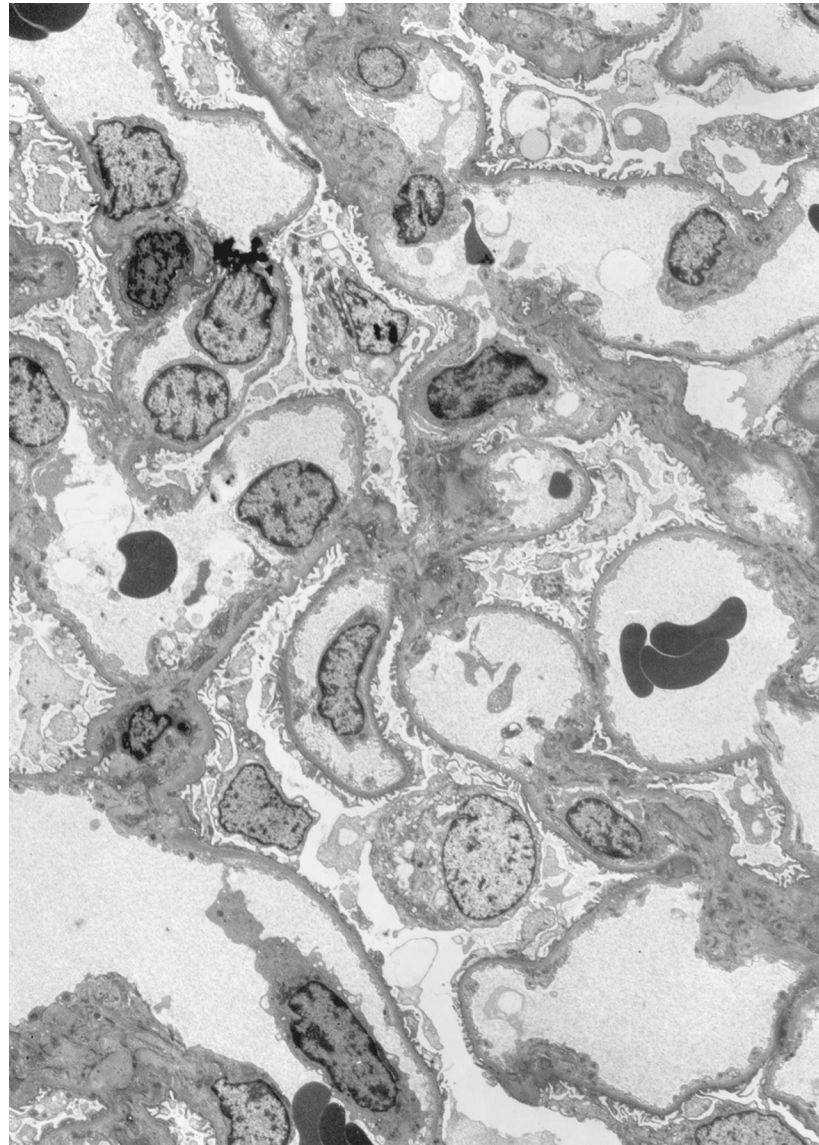


FIG. 2.5 This glomerulus shows only minimal abnormalities by electron microscopy, with rare vacuoles and blebs in the podocytes. The foot processes are largely intact. The glomerular basement membrane is of normal thickness. Red blood cells and rare platelet fragments are found within capillary lumina. The mesangial areas show mesangial cells surrounded by matrix (transmission electron microscopy, $\times 3000$).

parietal epithelial cells are normally present at the junction between flat epithelial cells and the cuboidal cells at the tubular junction. These cells may more readily be activated, as evidenced by increased staining with CD-44 and Ki-67, and contribute to tip lesions of focal segmental glomerulosclerosis (FSGS). Immature nephrons may occasionally be seen in the superficial cortex of children up to 1 year of age (Figs. 2.9–2.11; see also Figs. 2.6–2.8). There is no glomerulogenesis (i.e., growth of new additional glomeruli) after term birth in humans. Increase in glomerular volume, however, continues until adulthood, with the average normal glomerular diameter being approximately $95\ \mu\text{m}$ in young children (average age 2.2 years) and 140 to $160\ \mu\text{m}$ in adulthood. Thickening of the GBM also occurs normally with maturational growth. Normal ranges are from 220 to $260\ \text{nm}$ at age 1 year, 280 to $327\ \text{nm}$ at age 5 years, 329 to $370\ \text{nm}$ at age 10 years, and 358 to $399\ \text{nm}$ at age 15 years, the latter being similar to adult normal thickness (see Figs. 2.4 and 2.5). Global glomerulosclerosis may occur without renal disease as a part of normal maturation, aging, and repair. Less than 5% global glomerulosclerosis is expected in children and young adults and less than (age divided by 2, minus 10) percent in aged normal individuals.

TABLE 2.1 Definitions of Common Terms to Describe Morphologic Lesions**Light Microscopy**

Focal ^a	Involving some glomeruli
Diffuse ^a	Involving all glomeruli
Segmental	Involving part of glomerular tuft
Global	Involving total glomerular tuft
Lobular	Simplified, lobular appearance of capillary loop architecture because of endocapillary proliferation/hypercellularity (defined later) (seen in, for example, MPGN)
Nodular	Relatively acellular areas of mesangial matrix expansion producing rounded nodules (seen in, for example, diabetic nephropathy)
Glomerular sclerosis	Obliteration of capillary loop and increased matrix
Crescent	Proliferation of parietal epithelial cells
Spikes	Projections of GBM intervening between subepithelial immune deposits (seen in, for example, membranous nephropathy)
Endocapillary proliferation/hypercellularity	Proliferation of mesangial and/or endothelial cells or hypercellularity because of infiltrating inflammatory cells, filling up and distending capillary lumens (seen in, for example, lupus nephritis)
Hyaline	Descriptive of glassy, smooth-appearing material
Hyalinosis	Hyaline-appearing insudation of plasma proteins (seen in, for example, focal segmental glomerulosclerosis)
Mesangial area	Stalk region of capillary loop with mesangial cells surrounded by matrix
Subepithelial	Between podocyte and GBM
Subendothelial	Between endothelial cell and GBM
Tram-track	Double contour of glomerular basement because of deposits and/or circumferential interposition (see EM definitions later)
Wire loop	Thick, rigid appearance of capillary loop because of massive subendothelial deposits
Activity	Description encompassing possible treatment-sensitive lesions (e.g., extent of cellular crescents, cellular infiltrate, necrosis, proliferation)
Chronicity	Description of probable irreversible lesions (e.g., extent of tubular atrophy, interstitial fibrosis, fibrous crescents, sclerosis)

Immunofluorescence Microscopy

Granular	Discontinuous flecks of staining producing a granular pattern; seen along the capillary loop in membranous nephropathy
Linear	Smooth continuous staining, seen along capillary loop in, for example, anti-GBM antibody-mediated GN, or along TBM in anti-TBM nephritis

Electron Microscopy

Foot process effacement	Flattening of foot processes so that they cover the basement membrane, with loss of slit diaphragms
Microvillous transformation	Small extensions of visceral epithelial cells with villus-like appearance
Cellular interposition (CIP)	Extension of mesangial cell or infiltrating monocyte cytoplasm with interposition between endothelial cell cytoplasm and basement membrane, often with underlying new basement membrane formation
Reticular aggregates	Organized arrays of membrane particles within endothelial cells (also called tubuloreticular inclusions)
Immunotactoid GP	Large, organized microtubular deposits, >30 nm diameter
Fibrillary GN	Fibrils 14–20 nm diameter without organization

^aIn some classifications, “focal” is used to define lesions affecting <50% of glomeruli and “diffuse” lesions that affect ≥50% of glomeruli. EM, Electron microscopy; GBM, glomerular basement membrane; GN, glomerulonephritis; GP, glomerulopathy; MPGN, membranoproliferative glomerulonephritis; TBM, tubular basement membrane.

FIG. 2.6 During development, various stages of immature glomeruli may be found at different cortical levels within the kidney. The deep juxtamedullary glomeruli mature first. This immature glomerulus is from the midcortical level of a 28-week-gestation premature baby. There is prominent mesangium and very simple capillary branching with overlying plump, cuboidal glomerular visceral epithelial cells. The parietal epithelial cells lining Bowman's capsule are also more cuboidal than in the mature state (periodic acid Schiff, $\times 400$).

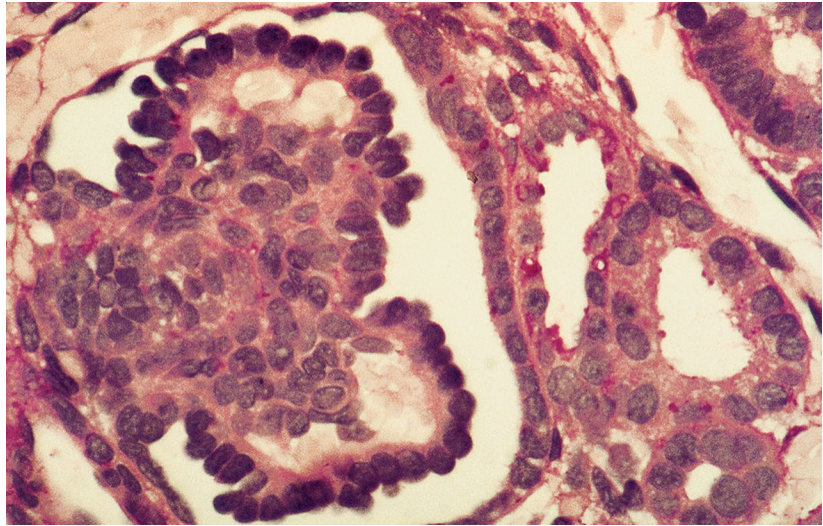


FIG. 2.7 These glomeruli are from the same 28-week-gestation baby as shown in Fig. 2.6. They have more complex capillary branching pattern but maintain immature, plump glomerular visceral epithelial cells. In one glomerulus (on the right), the parietal epithelial cells are flattened and more mature in appearance (periodic acid Schiff, $\times 200$).

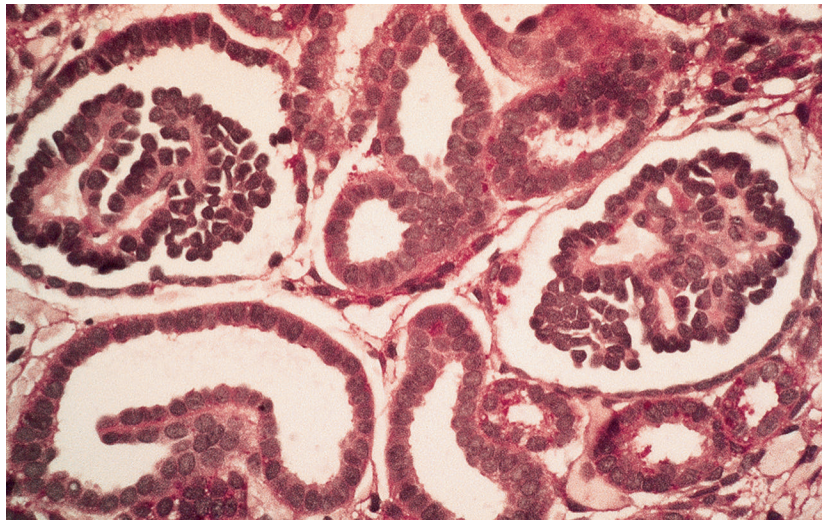
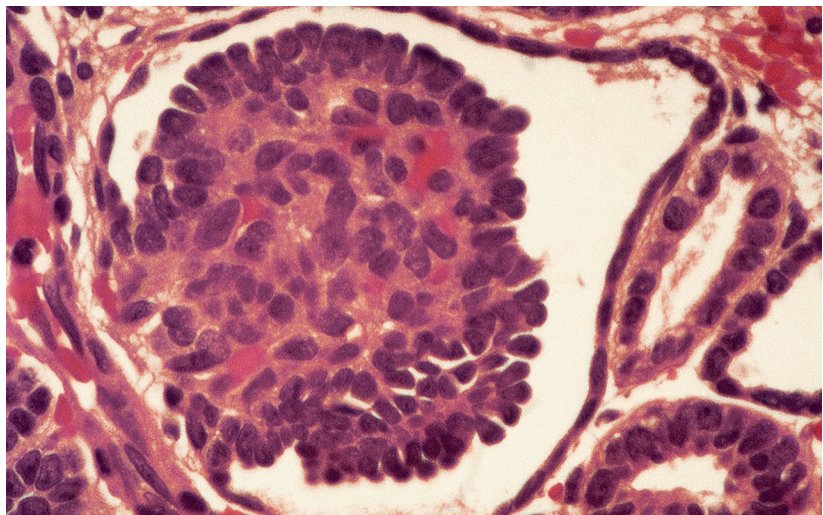


FIG. 2.8 This deep juxtamedullary glomerulus is from the same 28-week-gestation baby as shown in the previous figures. There is a complex capillary branching pattern with overlying plump, still immature glomerular visceral epithelial cells. Bowman's space is pouching out to form a junction with the proximal tubular epithelium on the right (periodic acid Schiff, $\times 400$).



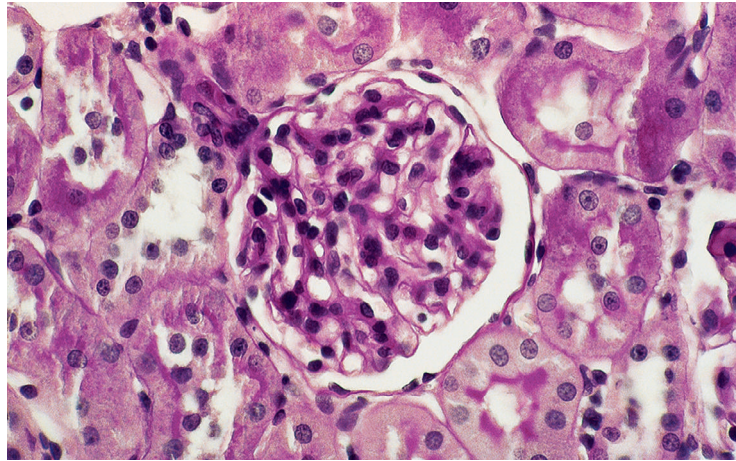


FIG. 2.9 The small but completely mature glomerulus of a normal term baby is illustrated, with complex capillary branching pattern and mature, pale-gray flattened podocytes overlying the capillary loops. The normal vascular pole is seen at the upper left. Normal proximal tubules with periodic acid Schiff–positive brush border with intervening peritubular capillaries are also illustrated. Although glomeruli do not increase in number with maturational growth, they increase in size. A normal glomerular diameter in a child less than 5 years old in our biopsy practice is less than 95 μm . Individual laboratories must establish their own normal parameters because fixation and processing conditions may influence this parameter (periodic acid Schiff, $\times 100$).

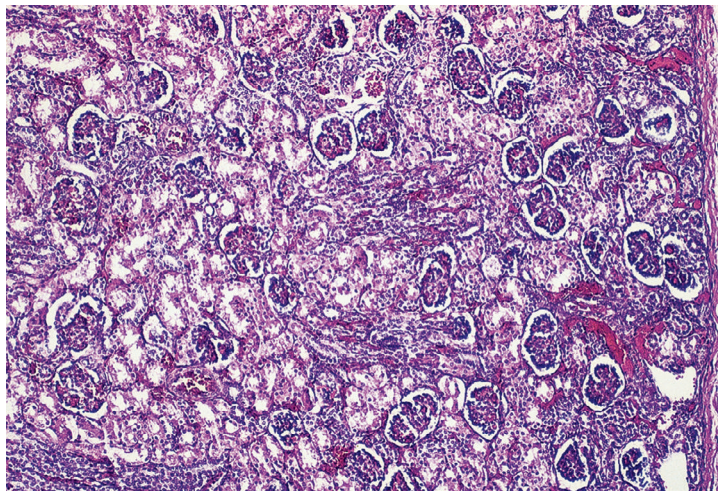


FIG. 2.10 The more superficial glomeruli (*right*) are less mature than the deeper juxtamedullary glomeruli (*left*) in this term infant. There is persistence of immature podocytes of the more superficial glomeruli, although capillary branching pattern is already complex (periodic acid Schiff, $\times 100$).

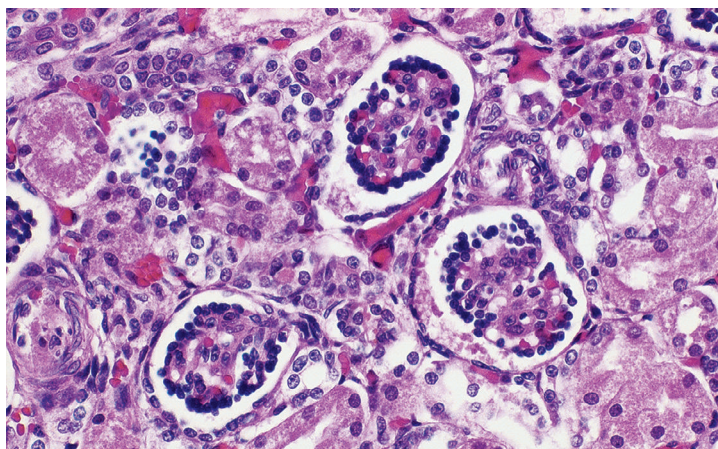


FIG. 2.11 Immature glomeruli from a 3-day-old infant show immature, plump cuboidal podocytes, with moderately complex capillary branching pattern of the glomerulus on the right and more simple branching pattern of the glomeruli on the left (periodic acid Schiff, $\times 100$).

Selected Reading

- Fogo A, Hawkins EP, Berry PL, et al. Glomerular hypertrophy in minimal change disease predicts subsequent progression to focal glomerular sclerosis. *Kidney Int.* 1990;38:115-123.
- Fogo AB, Kon V. The glomerulus—a view from the inside—the endothelial cell. *Int J Biochem Cell Biol.* 2010;42:1388-1397.
- Kaplan C, Pasternack B, Shah H, et al. Age-related incidence of sclerotic glomeruli in human kidneys. *Am J Pathol.* 1975;80:227-234.
- Kappel B, Olsen S. Cortical interstitial tissue and sclerosed glomeruli in the normal human kidney, related to age and sex. A quantitative study. *Virchows Arch A Pathol Anat Histol.* 1980;387:271-277.
- Kuppe C, Leuchtle K, Wagner A, et al. Novel parietal epithelial cell subpopulations contribute to focal segmental glomerulosclerosis and glomerular tip lesions. *Kidney Int.* 2019;96:80-93.
- Morita M, White RHR, Raafat F, et al. Glomerular basement membrane thickness in children. A morphometric study. *Pediatr Nephrol.* 1988;2:190-195.
- Shindo S, Yoshimoto M, Kuriya N, et al. Glomerular basement membrane thickness in recurrent and persistent hematuria and nephrotic syndrome: correlation with sex and age. *Pediatr Nephrol.* 1988;2:196-199.
- Smith SM, Hoy WE, Cobb L. Low incidence of glomerulosclerosis in normal kidneys. *Arch Pathol Lab Med.* 1989;113:1253-1256.

Glomerular Diseases

PRIMARY GLOMERULAR DISEASES, 16

Glomerular Diseases That Cause Nephrotic Syndrome: Nonimmune Complex, 16

Minimal Change Disease and Focal Segmental Glomerulosclerosis: Introduction, 16

Minimal Change Disease, 17

Focal Segmental Glomerulosclerosis, 20

Collapsing Glomerulopathy, 34

Tip Lesion Variant of Focal Segmental Glomerulosclerosis, 40

Cellular Variant of Focal Segmental Glomerulosclerosis, 42

Perihilar Variant of Focal Segmental Glomerulosclerosis, 44

Congenital Nephrotic Syndrome of Finnish Type, 46

Diffuse Mesangial Sclerosis, 49

Frasier Syndrome, 52

Glomerular Diseases That Cause Nephrotic/Nephritic Syndrome: Complement-Related, 54

C1q Nephropathy, 54

C3 Glomerulopathies, 56

Dense Deposit Disease, 57

C3 Glomerulonephritis, 64

Glomerular Diseases That Cause Nephrotic Syndrome Because of Deposits, 69

Membranous Nephropathy, 69

Membranoproliferative Glomerulonephritis, 85

Fibrillary Glomerulonephritis, 99

Immunotactoid Glomerulopathy, 107

Glomerular Diseases That Cause Hematuria or Nephritic Syndrome: Immune Complex, 111

Acute Postinfectious Glomerulonephritis, 111

Immunoglobulin A–Dominant Infection-Related Glomerulonephritis, 122

Immunoglobulin A Nephropathy, 127

SECONDARY GLOMERULAR DISEASES, 140

Diseases Associated With Nephrotic Syndrome, 140

Monoclonal Immunoglobulin Deposition Disease, 140

Amyloidosis, 155

Proliferative Glomerulonephritis With Monoclonal Deposits, 165

HIV-Associated Nephropathy, 169

Sickle Cell Nephropathy, 175

Fabry Disease, 182

Lipoprotein Glomerulopathy, 187

Lecithin-Cholesterol Acyltransferase Deficiency, 189

Hereditary Focal Segmental Glomerulosclerosis, 193

Diseases Associated With Nephritic Syndrome or Rapidly Progressive Glomerulonephritis: Immune-Mediated, 195

Lupus Nephritis, 195

Atypical Presentations of Renal Involvement in Systemic Lupus Erythematosus, 212

Immunoglobulin A Vasculitis (Henoch–Schönlein Purpura), 224

Mixed Connective Tissue Disease, 233

Mixed Cryoglobulinemia, 239

Anti–Glomerular Basement Membrane Antibody–Mediated Glomerulonephritis, 251

Diseases Associated With the Nephritic Syndrome or Rapidly Progressive Glomerulonephritis: Pauci-Immune- or Nonimmune-Mediated, 259

Antineutrophil Cytoplasmic Autoantibody–Associated Small-Vessel Vasculitis (Pauci-Immune Glomerulonephritis), 259

Microscopic Polyangiitis, 261

Granulomatosis With Polyangiitis (Wegener's Granulomatosis), 263

Eosinophilic Granulomatosis With Polyangiitis (Churg-Strauss Syndrome), 272

Polyarteritis Nodosa, 272

Diseases With Abnormal Collagen/Basement Membranes, 273

Alport Syndrome, 273

Thin Basement Membrane Lesions, 283

Nail-Patella Syndrome, 286

Type III Collagen Glomerulopathy, 288

Glomerular Involvement With Bacterial Infections, 291

Subacute Bacterial Endocarditis, 291

Shunt Nephritis, 297

Primary Glomerular Diseases

Glomerular Diseases That Cause Nephrotic Syndrome: Nonimmune Complex

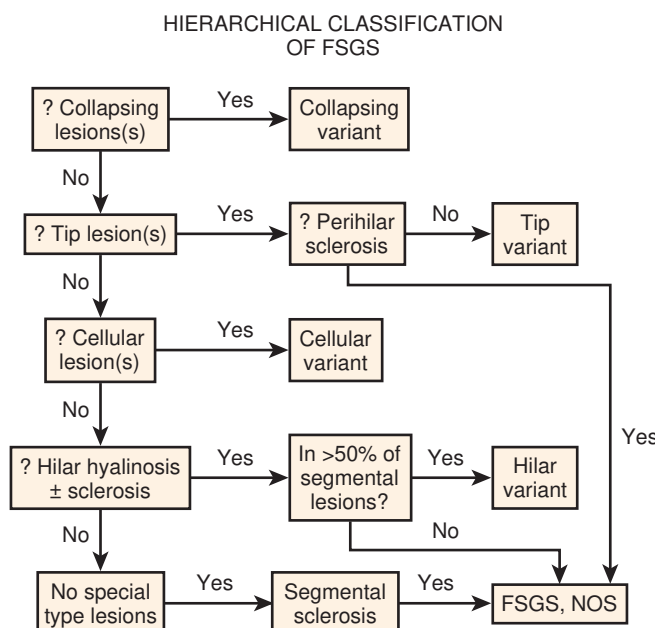
MINIMAL CHANGE DISEASE AND FOCAL SEGMENTAL GLOMERULOSCLEROSIS: INTRODUCTION

Minimal change disease (MCD) and focal segmental glomerulosclerosis (FSGS) both typically present as nephrotic syndrome and cannot be readily distinguished based solely on clinical presentation. Approximately 90% of children ages 1 to 7 years with nephrotic syndrome appear to have MCD, and the vast majority respond to steroids. Thus biopsy is only done if the child is unresponsive to steroids or has clinical features suggesting another etiology of the nephrotic syndrome. Among the minority of nephrotic children who were steroid unresponsive/dependent or had frequent relapses and therefore underwent kidney biopsy, FSGS was diagnosed in about 7%. In biopsied adolescents, FSGS is observed more commonly than MCD. In adults, MCD accounts for 10% to 15% of nephrotic syndrome. The term “FSGS” is unfortunately used both for a disease with primary injury to podocytes that appears mediated by a circulating factor and for any glomerular scarring lesion that occurs in a focal and segmental distribution. Primary podocytopathy-related FSGS has increased in incidence, and in the United States in adults has surpassed membranous nephropathy as a cause of nephrotic syndrome (18.7% incidence), especially in African Americans and Hispanics. Similar increased incidence of FSGS linked to ethnicity has also been reported in children with nephrotic syndrome. The incidence of FSGS is less in older adults. Serologic studies, including complement levels, are typically within normal limits in both MCD and FSGS. Renal biopsy is thus essential to determine the etiology of nephrotic syndrome in adults and also in children who are not steroid responders. The ultimate prognosis differs dramatically, with complete recovery the rule in MCD, contrasting with progressive renal insufficiency in FSGS. Several morphologic variants of FSGS have also been investigated for their prognostic significance. Of note, the morphologic subtypes are not specific for a primary etiology of FSGS lesions. The impact of these morphologic variants on prognosis was investigated in the National Institute of Health (NIH) FSGS Clinical Trials cohort of 138 patients with steroid-resistant primary FSGS, treated with mycophenolate mofetil and dexamethasone versus cyclosporine, with no difference

TABLE 3.1 Focal Segmental Glomerulosclerosis Variants

Type	Defining Feature
FSGS, not otherwise specified	Discrete segmental sclerosis
FSGS, perihilar variant	Perihilar sclerosis and hyalinosis
FSGS, cellular variant	Endocapillary hypercellularity
FSGS, tip variant	Sclerosis at tubular pole with adhesion at tubular lumen/neck
FSGS, collapsing variant (collapsing glomerulopathy)	Segmental or global collapse of tuft and visceral epithelial cell hyperplasia/hypertrophy

FSGS, Focal segmental glomerulosclerosis.

**FIG. 3.1** Hierarchical classification of focal segmental glomerulosclerosis.

in response between treatment groups. The morphologic variants of FSGS, however, were associated with differences in treatment responses, with worst outcome in those with collapsing variant and best in those with tip variant, with intermediate results for those with FSGS not otherwise specified (NOS). The Columbia working classification proposal is given in [Table 3.1](#) and the hierarchical relationship of the variants is shown in [Fig. 3.1](#). Each of the subtypes will be discussed later.

MINIMAL CHANGE DISEASE

MCD is named for the apparent structurally normal glomeruli by light microscopy ([Figs. 3.2–3.3](#)). There are no specific vascular or tubulointerstitial lesions in idiopathic MCD. Nevertheless, MCD may also occur in the middle-aged or older adult (10%–15% of nephrotic syndrome in adults) who has nonspecific focal areas of tubulointerstitial scarring and mild vascular lesions (arteriosclerosis, arteriolar hyaline related to hypertension, or other unrelated disease). Global glomerulosclerosis, in contrast to the segmental glomerular sclerotic lesion, is not of special diagnostic significance in considering the differential of MCD versus FSGS. Globally sclerotic glomeruli may be normally seen at any age, show an obsolescent pattern (see also “Age-Related Sclerosis,” in Chapter 7), and are thought to result from normal “wear and tear” and not specific disease mechanisms in most cases. Up to 10% of glomeruli may be normally globally sclerosed in people younger than 40 years of age. The extent of global sclerosis increases with aging, up to 30% by age 80 (estimated by calculating half the patient’s age minus 10).

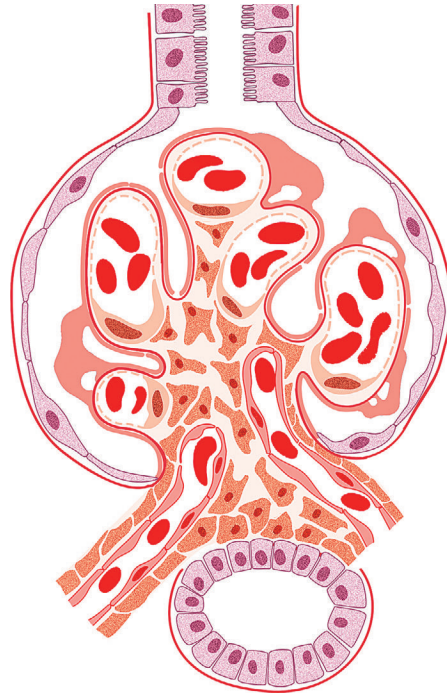


FIG. 3.2 Minimal change disease. The glomeruli are normal by light microscopy, but with diffuse effacement of foot processes by electron microscopy.

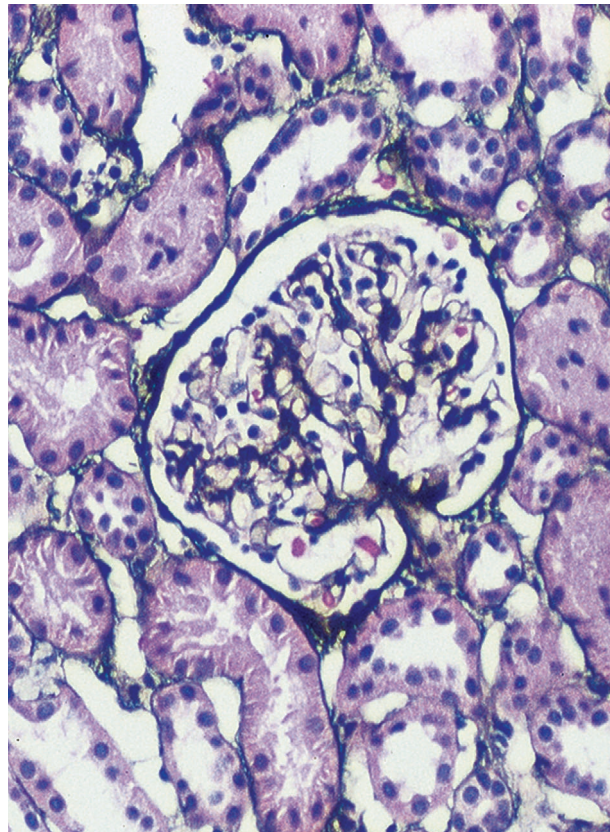


FIG. 3.3 Minimal change disease (MCD). Glomeruli appear unremarkable by light microscopy, and in young patients there is no tubulointerstitial fibrosis, as in this patient. In older patients, MCD may occur on a background of nonspecific scarring of the tubulointerstitium and even nonspecific global glomerulosclerosis (Jones silver stain, $\times 200$).

Glomerular MCD-type lesions with associated acute interstitial nephritis (AIN), which is characterized by edema and interstitial lymphoplasmacytic infiltrate, often with eosinophils, suggest a drug-induced hypersensitivity reaction. This combined syndrome of MCD and AIN is classically because of nonsteroidal antiinflammatory drugs (NSAIDs). This condition is usually reversible with discontinuation of the drug.

Immunofluorescence (IF) studies are typically negative in MCD. The presence of immunoglobulin M (IgM) staining in otherwise apparent MCD biopsies has been a source of previous controversy, with some authors considering this a specific entity known as “IgM nephropathy” (see later).

Electron microscopy (EM) shows extensive foot process effacement, vacuolization, and microvillous transformation of podocytes in MCD (Figs. 3.4–3.5). Patients who have been treated with immunosuppression with partial or complete response before biopsy may show less or even no significant foot process effacement.

Etiology/Pathogenesis

The pathogenesis of MCD appears related to interactions of abnormal cytokines and podocytes that only affect glomerular permeability and do not promote sclerogenic mechanisms. Dysregulated interaction of T-cells via cytotoxic T lymphocyte antigen-4 (CTLA-4) with podocyte CD80 has been postulated, but not proven, to contribute to MCD. T helper type 2 cells may release interleukin (IL)-13, which in experimental studies increased CD80 on podocytes with foot process effacement and proteinuria ensuing. MCD has been associated with drug-induced hypersensitivity reactions, and can be triggered by, for example, NSAIDs (see earlier). MCD also has been associated with Hodgkin's lymphoma, bee stings, and other venom exposure and after viral or, rarely, other infection or atopic episodes, implicating immune dysfunction as an initiating factor. In most cases, the triggers for initial disease or relapses remain unknown. In some patients with lupus nephritis (LN) or IgA nephropathy (IgAN; see specific sections), limited mesangial deposits are associated with extensive foot process effacement and marked proteinuria, possibly representing an MCD-like injury related to the underlying immune complexes, or less likely, coincidental occurrence of two separate diseases.

Selected Reading

D'Agati VD, Kaskel FJ, Falk RJ. Focal segmental glomerulosclerosis. *N Engl J Med*. 2011;365:2398–2411.

Fogo AB. Causes and pathogenesis of focal segmental glomerulosclerosis. *Nat Rev Nephrol*. 2015;11:76–87.

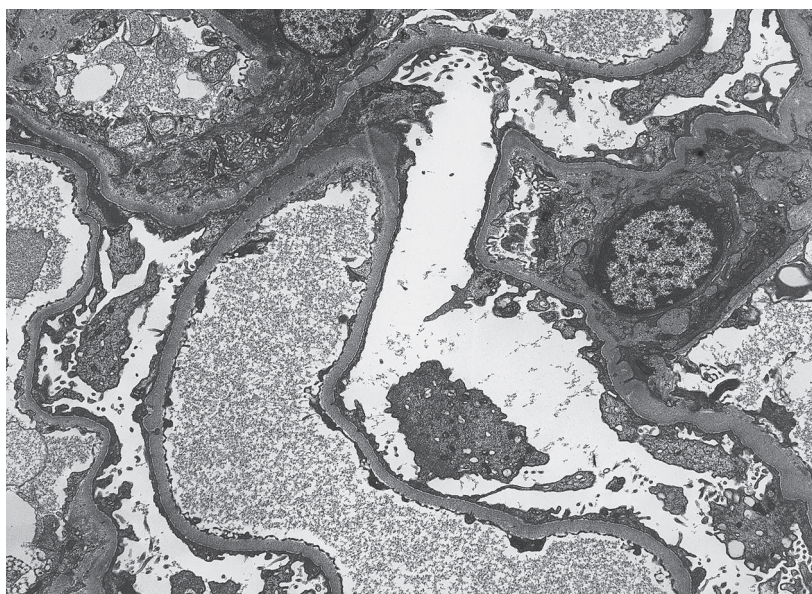


FIG. 3.4 Minimal change disease (MCD). Foot process effacement is extensive, often complete, in MCD, although the extent of foot process effacement cannot be used as a definitive criterion to differentiate this entity from focal segmental glomerulosclerosis. The glomerular basement membrane is unremarkable, and there are no deposits (transmission electron microscopy, $\times 3000$).

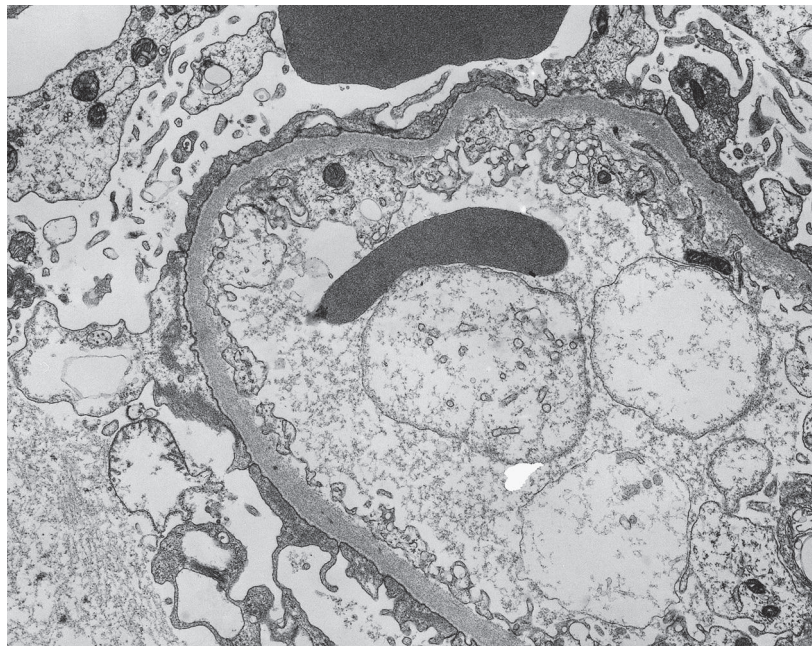


FIG. 3.5 Minimal change disease (MCD). Extensive foot process effacement and microvillous transformation of visceral epithelial cells in MCD. Although the endothelial cells are mildly swollen, the glomerular basement membrane is unremarkable, and there are no deposits (transmission electron microscopy, $\times 8000$).

Gulati S, Sharma AP, Sharma RK. et al. Changing trends of histopathology in childhood nephrotic syndrome. *Am J Kidney Dis.* 1999;3:646–650.

Kaneko K, Tsuji S, Kimata T, Kitao T, Yamanouchi S, Kato S. Pathogenesis of childhood idiopathic nephrotic syndrome: A paradigm shift from T-cells to podocytes. *World J Pediatr.* 2015;11:21–28.

FOCAL SEGMENTAL GLOMERULOSCLEROSIS

In FSGS of usual type (NOS; [Table 3.1](#)), sclerosis involves some, but not all, glomeruli (focal), and the sclerosis affects a portion of, but not the entire, glomerular tuft (segmental; [Figs. 3.6–3.7](#)). The morphologic diagnosis of FSGS is a light microscopic description of this pattern of scarring, which may occur in many settings. Differentiation of MCD (see earlier) from FSGS relies on a large enough sample to detect the sclerotic glomeruli because the detection of even a single glomerulus involved with segmental sclerosis is sufficient to invoke a diagnosis of FSGS rather than MCD. Thus it is apparent that the distinction of MCD and FSGS may be difficult, especially with the smaller samples obtained with current biopsy guns and smaller needles. A sample of only 10 glomeruli has a 35% probability of missing a focal lesion that affects 10% of the nephrons, decreasing to 12% if 20 glomeruli are sampled. The initial sclerosis is in the juxtamedullary glomeruli, and this region should be included in the sample (see [Fig. 3.7](#)). Conversely, sampling on one section by definition cannot identify all of the focally and segmentally distributed scars. Three-dimensional (3D) studies examining serial sections of glomeruli in cases of idiopathic FSGS have demonstrated that the process indeed is focal; that is, glomeruli without any sclerosis exist even when disease is well established ([Figs. 3.8–3.9](#)).

Because of these limitations in detection of sclerotic lesions, other diagnostic features in glomeruli uninvolved by the sclerotic process have been sought to suspect FSGS even without sclerosed glomeruli. Abnormal glomerular enlargement (see later) appears to be an early indicator of the sclerotic process even before overt sclerosis can be detected. The presence of marked glomerular enlargement in a biopsy of otherwise apparent MCD would therefore rather suggest an early, incipient stage of FSGS. Dystroglycan, a component of normal glomerular basement membrane (GBM) that contributes to podocyte–matrix interaction, is generally maintained in nonsclerotic segments in FSGS and decreased in MCD (but also in collapsing type FSGS). This marker, or other emerging biomarkers

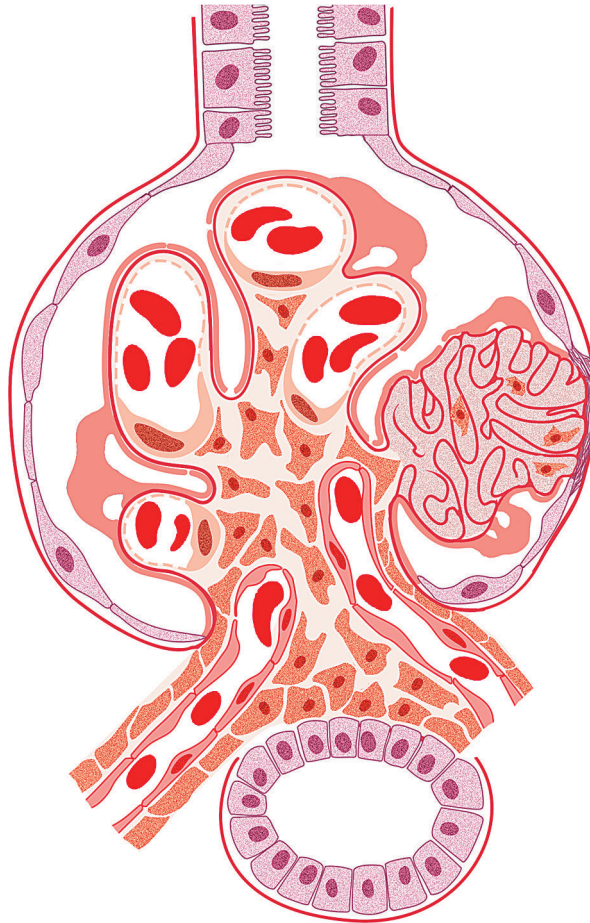


FIG. 3.6 Focal segmental glomerulosclerosis. There is sharply defined segmental sclerosis, defined as obliteration of capillary loops and increased matrix, without deposits and with diffuse foot process effacement by electron microscopy. Adhesions can also be present.

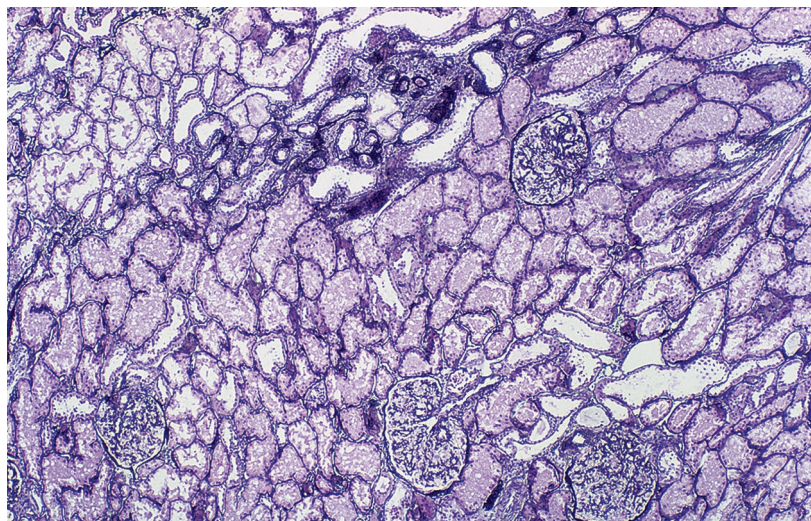


FIG. 3.7 Focal segmental glomerulosclerosis (FSGS). Early in FSGS, lesions are very focal, involving initially the juxtamedullary glomeruli. Tubulointerstitial fibrosis in a given section may be a clue to adjacent early segmental sclerotic lesions, which can be detected by careful serial section examination. In this field, one of four glomeruli (*top*) shows early segmental sclerosis of usual type, with an adjacent area of tubulointerstitial fibrosis (Jones silver stain, $\times 100$).

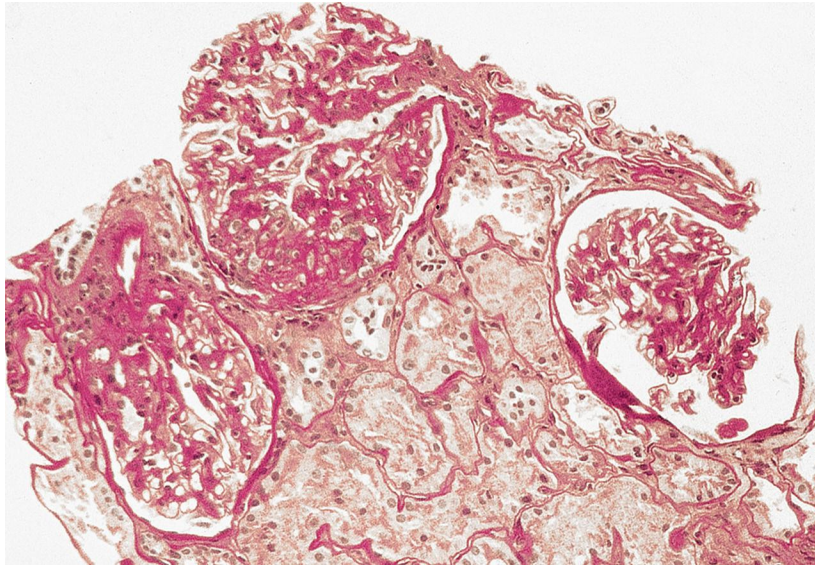


FIG. 3.8 Focal segmental glomerulosclerosis (FSGS). There is early segmental sclerosis that involves the periphery in one glomerulus (*top*), and the hilar area in another glomerulus (*left*), but without significant hyalinosis. This mixed pattern of sclerosis is characteristic of FSGS (periodic acid–Schiff, $\times 200$).

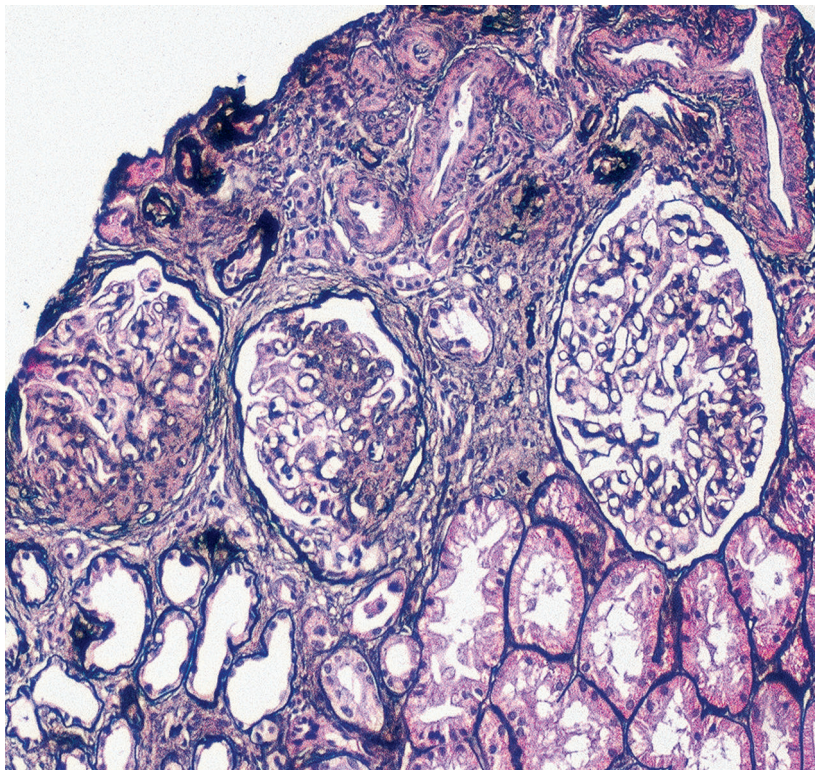


FIG. 3.9 Focal segmental glomerulosclerosis (FSGS). There are more advanced segmental sclerotic lesions affecting two of the three glomeruli in this field, with surrounding proportionate tubulointerstitial fibrosis. The sclerosis is characterized by increased matrix and obliteration of capillary lumens and is of the usual type of FSGS (Jones silver stain, $\times 200$).

from molecular and proteomic studies, although not completely sensitive or specific, may be of aid in favoring unsampled FSGS versus MCD in a biopsy with extensive foot process effacement and no defining segmental lesion. CD44 has emerged as one such marker. It is expressed in lymphocytes and in activated parietal epithelial cells. CD44 positive visceral epithelial cells were detected on the glomerular tuft in early recurrent FSGS in the transplant at the stage of foot process effacement, even before detectable sclerosing lesions, and also in early FSGS lesions in native kidneys. Activated parietal epithelial cells are postulated to migrate to the tuft, where they may in this setting contribute to sclerosis, producing the specific matrix LKIV69. Staining for LKIV69 aided in detection of very early segmental sclerotic lesions in native kidney biopsies. In contrast, in MCD, CD44 expression in this location was exceedingly rare. Diffuse mesangial hypercellularity may be a morphologic feature superimposed on changes of either MCD or FSGS, with or without IgM deposits, without defined prognostic significance (see later).

The periodic acid–Schiff (PAS)-positive acellular material in the segmental sclerotic lesions of the glomerulus may have different composition depending on the diverse pathophysiologic mechanisms discussed later. The sclerotic process is defined by glomerular capillary obliteration with increase in matrix, and varies from small, early lesions to near global sclerosis (Figs. 3.10–3.13). The segmental sclerosis lesions are discrete and may be located in perihilar and/or peripheral portions of the glomerulus. There may be associated global glomerulosclerosis of obsolescent type (see “Age-Related Sclerosis,” Chapter 7), which has no specific diagnostic significance. Uninvolved glomeruli show no apparent lesions by light microscopy but may appear enlarged, as do glomeruli with early-stage segmental sclerosis. The glomerulosclerosis may be associated with hyalinosis, resulting from insudation of plasma proteins, producing a smooth, glassy (hyaline) appearance (Fig. 3.14). This occurs particularly in the axial, vascular pole region. Of note, arteriolar hyalinosis may occur with hypertension-associated injury and should not be taken per se as evidence of a glomerular sclerotic lesion (see hilar-type FSGS, discussed later). Vascular sclerosis may be prominent late in the course of FSGS. Adhesion of the glomerular tuft to Bowman’s capsule (synechiae) is an early manifestation of sclerosis (Fig. 3.15). Glomerulosclerosis, when fully established, is accompanied by tubular atrophy, interstitial fibrosis with interstitial lymphocytes, proportional to the degree of scarring in the glomeruli (see Fig. 3.11). Of note, in HIV-associated nephropathy (HIVAN) and collapsing glomerulopathy, tubular lesions are often microcystic and disproportionately severe (see later).

IF may show nonspecific entrapment of IgM and C3 in sclerotic areas or areas where the mesangial matrix is increased (Fig. 3.16).

Electron microscopy shows extensive foot process effacement, even in glomeruli without a segmental sclerosing lesion (Fig. 3.17). Thus extent of foot process effacement does not allow precise distinction between MCD and FSGS in individual cases. Foot process effacement tends to be more extensive in primary FSGS compared with secondary FSGS; however, the overlap between these two categories does not allow one to use this as a diagnostic feature in individual cases. Secondary FSGS

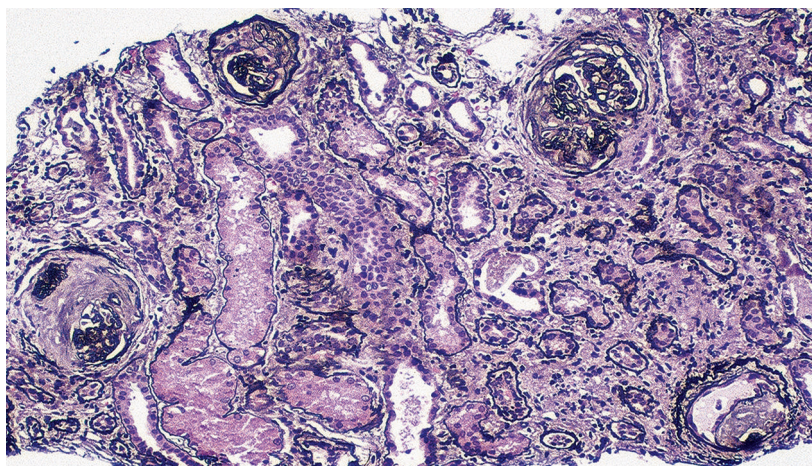


FIG. 3.10 Focal segmental glomerulosclerosis (FSGS). Near end-stage FSGS is present, with global or near global sclerosis of all glomeruli and extensive tubulointerstitial fibrosis and vascular thickening (Jones silver stain, $\times 200$).

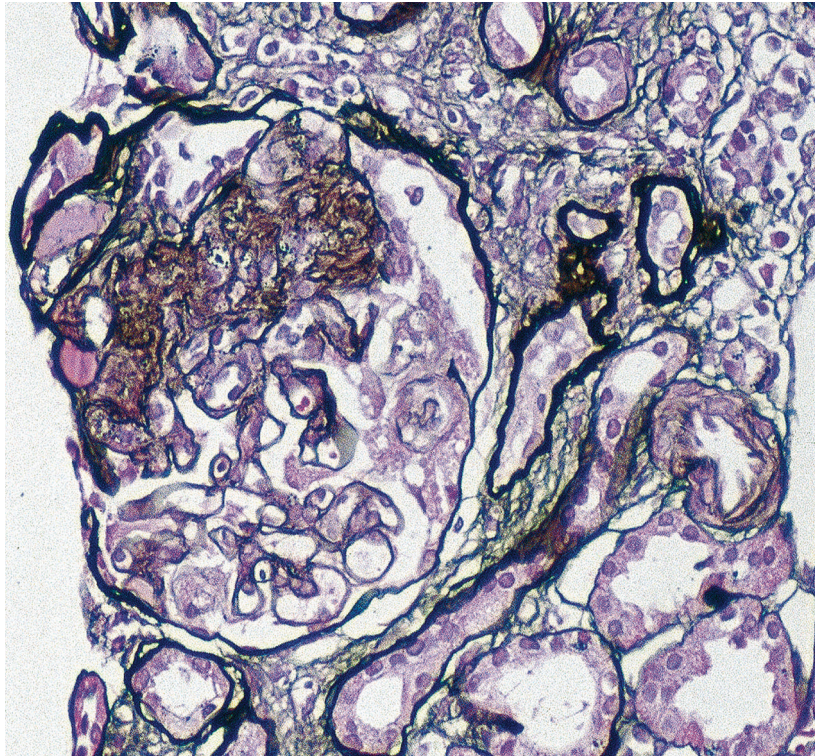


FIG. 3.11 Focal segmental glomerulosclerosis (FSGS). The typical segmental sclerotic lesion in FSGS is characterized by increased matrix and obliteration of capillary lumina, frequently with hyalinosis and adhesions, as illustrated here. There is surrounding tubulointerstitial fibrosis. The uninvolved segment of the glomerulus appears unremarkable (Jones silver stain, $\times 200$).

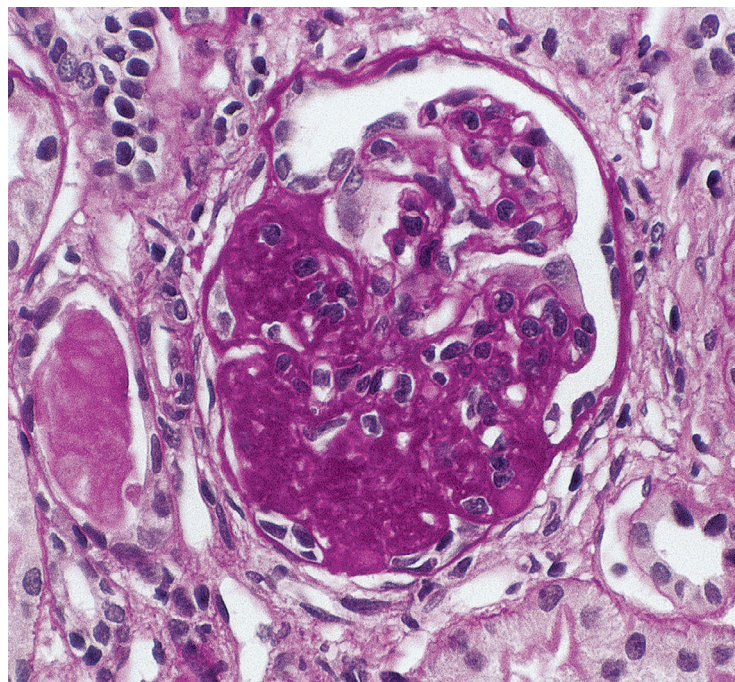


FIG. 3.12 Focal segmental glomerulosclerosis (FSGS). An advanced segmental sclerotic lesion of FSGS is shown, with only minimal hyaline droplets. There is increased mesangial matrix and obliteration of capillary lumina involving the majority of the glomerulus. The uninvolved portion of the glomerulus has mild increase in mesangial matrix. The adjacent tubule shows atrophy and a proteinaceous cast (periodic acid-Schiff, $\times 400$).

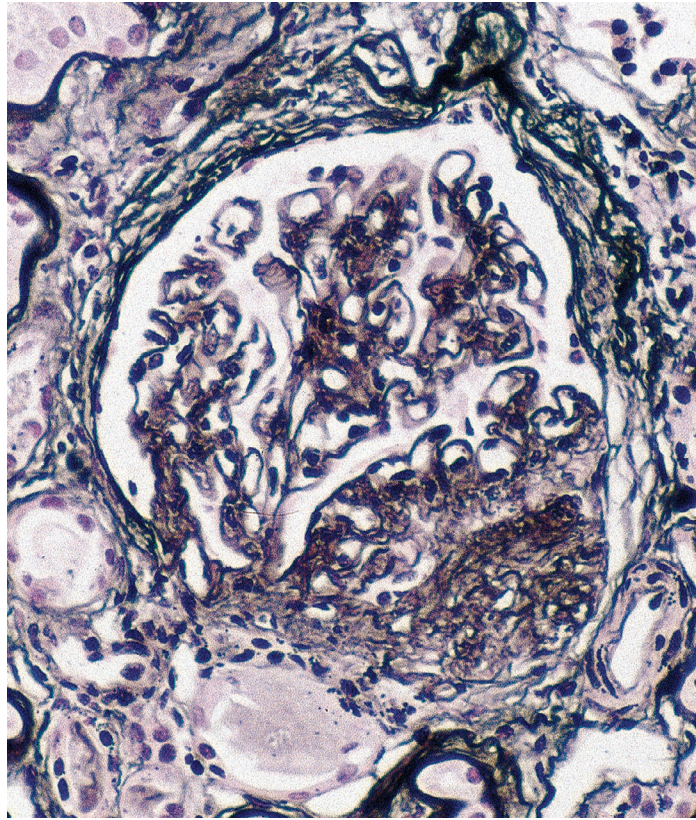


FIG. 3.13 Focal segmental glomerulosclerosis (FSGS). The segmental sclerotic lesion of FSGS is illustrated, with increased mesangial matrix and obliteration of capillary lumina. The remnants of the glomerular basement membrane in the sclerotic segment can be seen as wrinkled lines on this silver stain. The uninvolved portion of the glomerulus shows minimal mesangial matrix increase. Although this sclerotic lesion involves the vascular pole, there is no associated hyalinosis and the majority of segmental lesions were not hilar; the lesion is therefore classified as FSGS, not otherwise specified (Jones silver stain, $\times 400$).

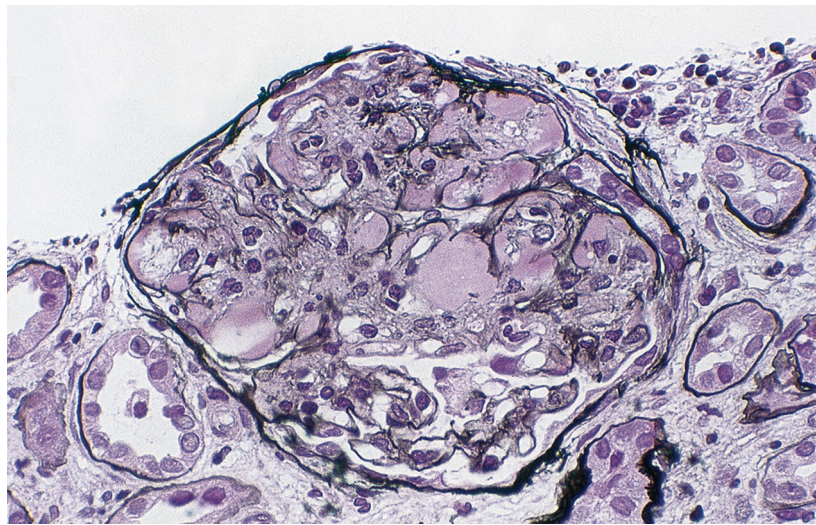


FIG. 3.14 Focal segmental glomerulosclerosis (FSGS). In this case of FSGS, there was extensive hyalinosis in the sclerotic areas, which are characterized by increased mesangial matrix and obliteration of capillary lumina. There are also adhesions of the sclerotic segments to Bowman's capsule, with thickened and disrupted Bowman's capsule. The hyalinosis represents an insudation of plasma proteins, reflecting endothelial injury (Jones silver stain, $\times 400$).

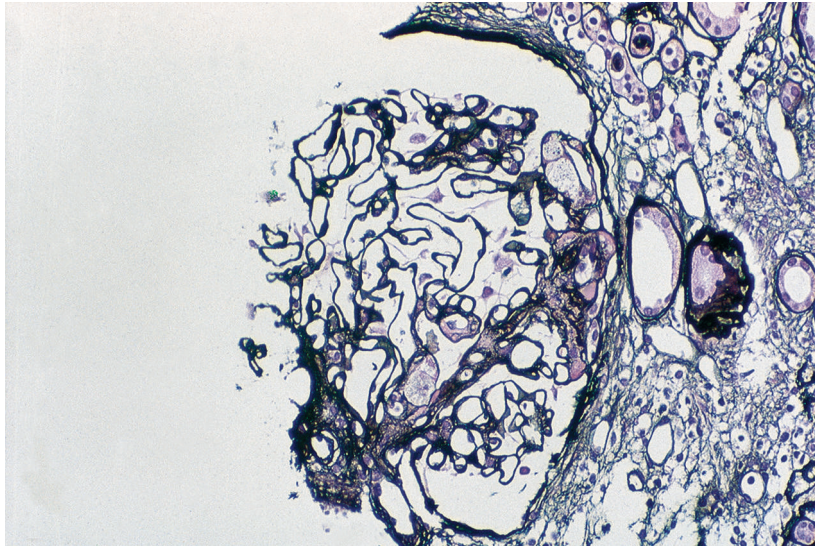


FIG. 3.15 Focal segmental glomerulosclerosis (FSGS). Early lesion of FSGS with adhesion of glomerular tuft to Bowman's capsule and small segmental area of hyalinosis and intracapillary foam cells (Jones silver stain, $\times 400$).

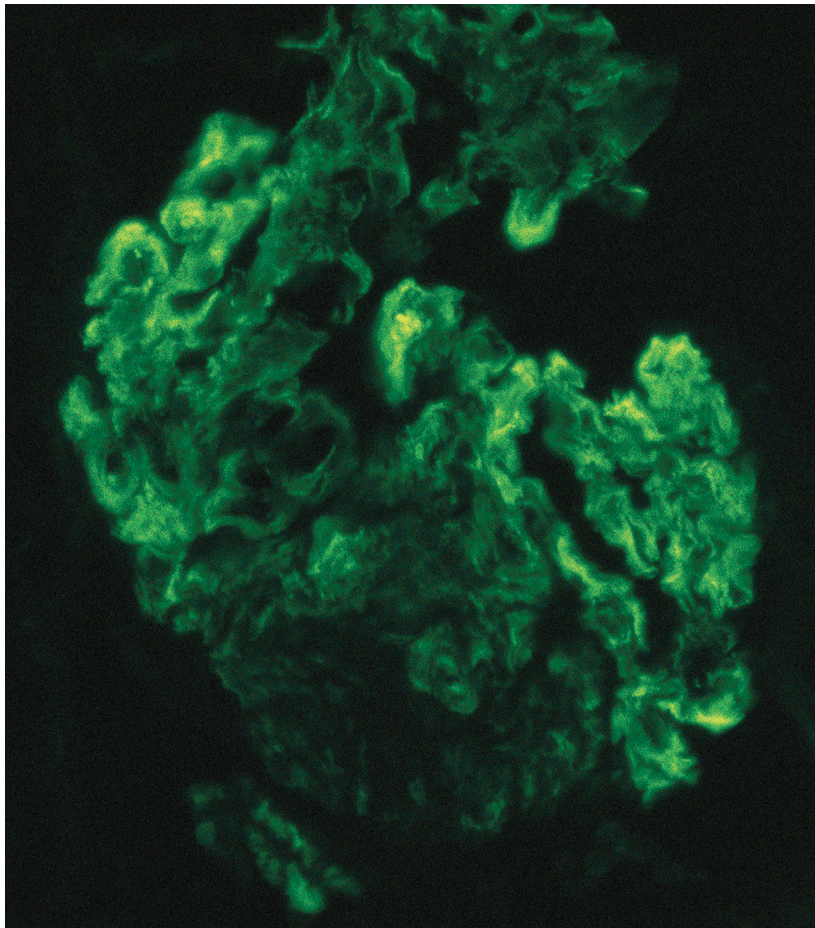


FIG. 3.16 Focal segmental glomerulosclerosis (FSGS). Immunofluorescence studies in FSGS do not show immune complexes but may show immunoglobulin M (IgM) in sclerotic areas or in areas of mesangial expansion (anti-IgM antibody immunofluorescence, $\times 400$).

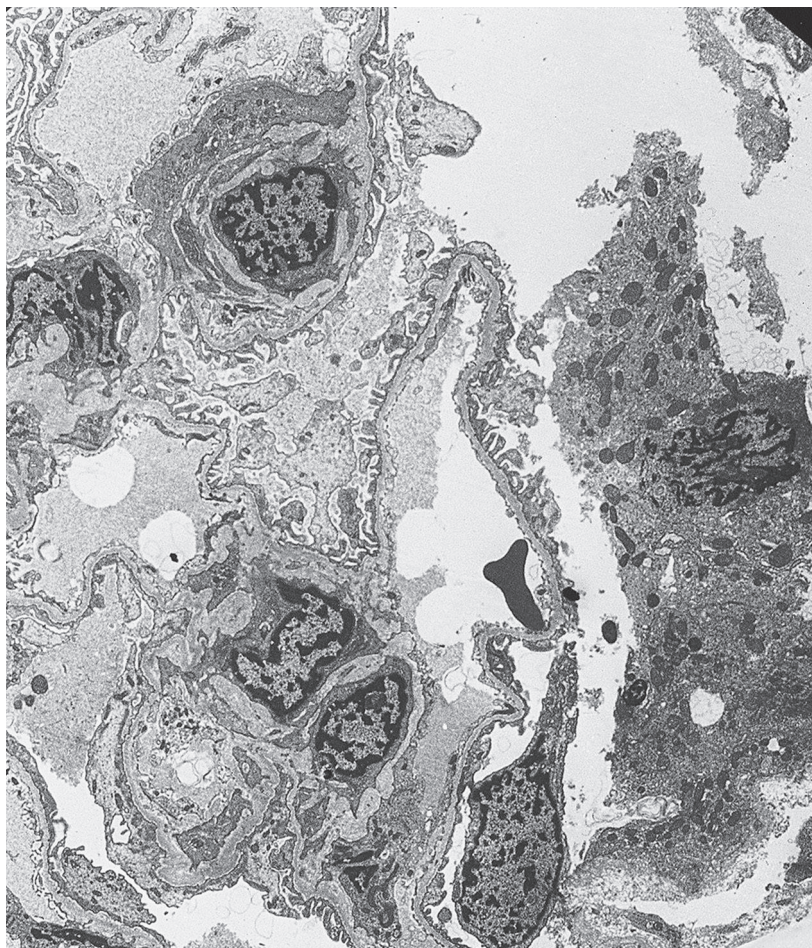


FIG. 3.17 Focal segmental glomerulosclerosis (FSGS). By electron microscopy, there is extensive foot process effacement in FSGS. Nevertheless, it may not be complete, as illustrated here. If there is less than approximately 50% foot process effacement, the diagnosis of primary FSGS is in doubt. There is also mesangial matrix expansion, without immune deposits (transmission electron microscopy, $\times 3000$).

lesions may show extensive foot process effacement in glomeruli affected by the segmental sclerosing process. Conversely, the absence of significant (i.e., less than 50%) foot process effacement should cast doubt on the diagnosis of untreated primary, idiopathic FSGS. There are no immune deposits in idiopathic FSGS, but mesangial matrix is increased in sclerotic areas (Fig. 3.18). Areas of hyaline may be present in the sclerotic segments and appear dense by EM but should be readily recognized as hyaline, and not confused with immune complexes, by observing scattered lipid droplets and correlating with scout section light microscopic appearance (Fig. 3.19). The presence of numerous reticular aggregates in endothelial cells in the setting of segmental glomerulosclerosis with collapsing features suggests possible HIVAN (see later). Reticular aggregates have also been observed in some patients with severe acute respiratory syndrome coronavirus 2 (SARS-CoV-2) infection and collapsing glomerulopathy, likely linked to enhanced cytokine release in these patients.

Diagnosis of Recurrence of Focal Segmental Glomerulosclerosis in the Transplant

So-called “primary” FSGS recurs in 30% to 40% of patients. Most recurrences occur within the first months after transplantation. Proteinuria may recur immediately after the graft is implanted, implicating circulating factor(s) in the recurrence. Foot process effacement is present at the time of recurrence of proteinuria and precedes the development of sclerosis, typically by weeks to months. Glomerular enlargement at this stage of recurrent FSGS is prominent in children who otherwise do not undergo glomerular enlargement when receiving an adult kidney. In contrast, an adult recipient of a single

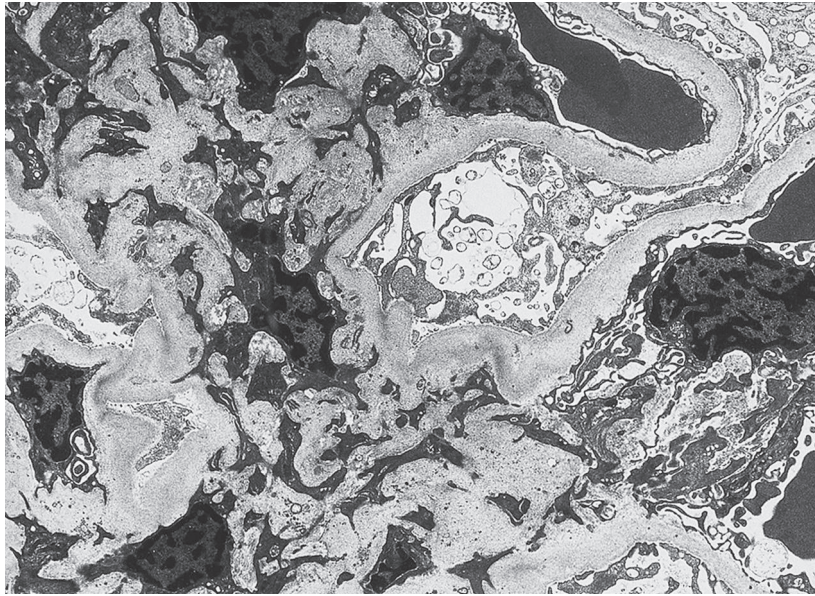


FIG. 3.18 Focal segmental glomerulosclerosis (FSGS). Segmental increase in matrix with obliterated capillary lumens is apparent in this case of FSGS. The overlying visceral epithelial cells show vacuolization, microvillous transformation, and extensive foot process effacement. The corrugated, collapsed glomerular basement membrane is evident. There are no immune deposits (transmission electron microscopy, $\times 5000$).

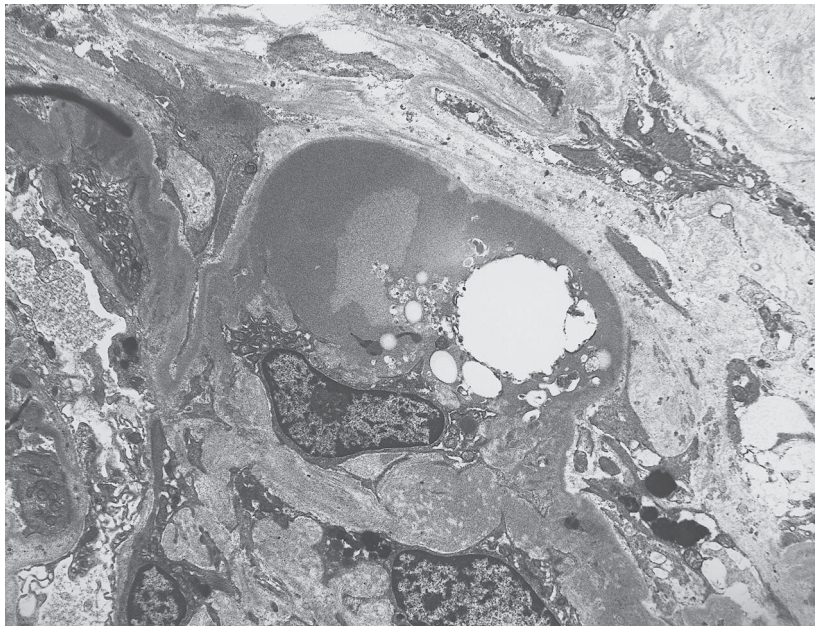


FIG. 3.19 Focal segmental glomerulosclerosis (FSGS). Hyaline deposit within a segmentally sclerotic area in FSGS. Hyaline is smooth, homogeneous, usually located in areas of sclerosis, and frequently contains lipid (clear, round areas). The sclerotic segment is characterized by increased matrix and obliteration of the capillary lumen, with dense adhesion to the overlying fibrotic Bowman's capsule (transmission electron microscopy, $\times 3000$).

kidney will normally have marked renal and glomerular growth to provide adequate glomerular filtration rate (GFR). Overt sclerosis is not noted until weeks to even months after recurrence of nephrotic syndrome. Thus during this time interval in the setting of the FSGS patient with nephrotic syndrome in the transplant, foot process effacement alone, even without detectable segmental sclerosis, is evidence of recurrent FSGS. Activated parietal epithelial cells, staining for CD44, are increased on the glomerular tuft itself even in this early phase of recurrent FSGS and are postulated to have migrated from Bowman's capsule. Recurrent FSGS often, but not invariably, shows a similar phenotype as diagnosed by the Columbia classification of FSGS to what the patient had in their native kidney.

Differential Diagnosis of Minimal Change Disease Versus Focal Segmental Glomerulosclerosis

Some investigators have felt that the common clinical presentation and similar findings in intact glomeruli indicate that MCD and FSGS are two manifestations of the same disease. Our data and those from others rather support differences even at the earliest time points. CD44 is one such marker differentially expressed in visceral epithelial cells in FSGS versus MCD (discussed previously). Parietal epithelial cell-derived matrix LKIV69 expressed on the tuft is an additional useful marker to diagnose early FSGS. Much evidence has pointed to the participation of abnormal glomerular adaptation and growth factors in the pathogenesis of glomerulosclerosis. Several studies have shown that glomerular enlargement precedes overt glomerulosclerosis, in both pediatric and adult patients who otherwise had apparent MCD initially. Patients with abnormal glomerular growth, even on initial biopsies that did not show overt sclerotic lesions, subsequently developed overt glomerulosclerosis, as documented in later biopsies. A cut-off of greater than 50% larger glomerular area than normal for age was a sensitive indicator of increased risk for progression in one series of children with nephrotic syndrome. Of note, glomeruli grow in size until approximately 18 years of age, although no new glomeruli are formed after birth, so age-matched controls must be used in the pediatric population to assess normal glomerular size.

The finding of mesangial hypercellularity (>80% of glomeruli with more than three cells per mesangial region) has been proposed to indicate a subgroup of patients with poorer prognosis and increased risk for developing FSGS. Lack of uniform application of criteria for morphologic definition of mesangial hypercellularity makes it difficult to assess the impact of this feature on prognosis. Nevertheless, several series have failed to confirm a definite clinical correlation of this morphologic variant. Thus patients with mesangial hypercellularity in renal biopsies that otherwise show apparent MCD ultimately had good prognosis despite decreased initial response to steroids. Children with FSGS and mesangial hypercellularity did not show worse prognosis than those with typical FSGS. Thus diffuse mesangial hypercellularity does not appear to impart a specific prognostic significance in either MCD or FSGS, nor does it differentiate between apparent MCD and unsampled FSGS.

IgM deposits by IF in association with mesangial hypercellularity may indicate a poorer response to steroids, and some patients have shown histologic FSGS on second biopsy after an initial biopsy showed IgM nephropathy; however, the significance of IgM deposits by IF in the setting of normal glomeruli by light microscopy has been difficult to assess. Again, series of biopsies from children with FSGS and nephrotic syndrome have failed to show a specific predictive value of the IgM staining with or without diffuse mesangial hypercellularity. If deposits are present by EM and by IF, a mesangio-pathic/mesangioproliferative immune complex glomerulonephritis (GN) should be diagnosed.

In summary, the diagnosis of FSGS cannot be completely excluded when segmental sclerotic lesions are not detected, even with a biopsy of adequate size. It is therefore best to include the possibility of unsampled FSGS in biopsies from patients with nephrotic syndrome, no immune complexes, and extensive foot process effacement, especially when glomerular number is less than 25, or other morphologic findings indicative of probability of unsampled FSGS are present. These include glomerular enlargement and interstitial fibrosis (in young patients), and possibly preserved Dystroglycan staining, the parietal epithelial cell-derived matrix LKIV69, or CD44-positive epithelial cells on the glomerular tuft.

Etiology/Pathogenesis

Primary FSGS is thought to result from an undefined circulating factor or factors that mediate abnormal glomerular permeability and ultimately sclerosis. Soluble urokinase plasminogen activator receptor (suPAR) and cardiotrophin-like cytokine-1 (CLC-1) have been postulated to represent such causative

circulating factors. suPAR, however, is increased with decreased GFR, regardless of cause, and is increased in a variety of inflammatory conditions without FSGS. Inactivation of CLC-1 by galactose infusion has not prevented recurrent FSGS. Thus a proven causal circulating factor in FSGS has not been definitively identified. Recent studies have pointed to podocyte injury and dedifferentiation of its phenotype, with loss of podocytes, with activated parietal epithelial cell migration to the tuft, in the pathogenesis of the sclerotic lesions. The finding of CD44-positive cells, a marker of such activated parietal epithelial cells, on the glomerular tuft precedes overt sclerosing lesions in recurrent FSGS in the transplant, and CD44 or matrix LKIV69 staining on the tuft could also enhance recognition of early sclerosing lesions in native kidneys.

Expanded understanding of the molecular biology of the podocyte and identification of genes mutated in rare familial forms of FSGS (e.g., *ACTN4*, *NPHS2*, which encodes podocin, *TRPC-6*, *PLCE1*, *INF-2*, *WT1*, *CD2AP*, *LAMB2*), or in congenital nephrotic syndrome of Finnish type (nephrin, coded by the *NPHS1* gene), have given important new insights into the mechanisms of progressive glomerulosclerosis and nephrotic syndrome. Genetic studies of familial nephrotic syndrome/FSGS show a high yield of detection of pathogenic or possibly pathogenic mutations in younger patients. Thus in children less than 1 year old with steroid-resistant FSGS, 50% had mutations detected, decreasing to 25% in children between the ages of 1 and 6, and even less in older children and adolescents (18% and 11%, respectively). With increasing age of onset of FSGS and in nonfamilial cases, the detection of causal mutations is substantially less, about 8% in adult sporadic FSGS in one series. We will only briefly discuss some of these genetic forms of FSGS. Key gene mutations causing FSGS/nephrotic syndrome include those encoding structural proteins of the podocyte cytoskeleton or slit diaphragm, those governing podocyte–GBM interaction, affecting mitochondrial function, or coenzyme Q10 function (*COQ*). Nephrin localizes to the slit diaphragm of the podocyte and is tightly associated with CD2-associated protein (CD2AP). Nephrin functions as a zona occludens–type junction protein and, along with CD2AP, plays a crucial role in receptor patterning, cytoskeletal polarity, and signaling. Mice engineered to be deficient in CD2AP develop congenital nephrotic syndrome, similar to congenital nephrotic syndrome of Finnish type (CNF). Autosomal dominant FSGS can be caused by mutations in one of several genes, including alpha-actinin 4 (*ACTN4*; Figs. 3.20–3.21). This is hypothesized to cause altered actin cytoskeleton interaction, perhaps causing FSGS through a gain-of-function mechanism, contrasting with the loss-of-function mechanism implicated for disease caused by the nephrin mutation mice, with either knockout or knock-in of mutated *ACTN4* that develop FSGS lesions. Thus balance of *ACTN4* is crucial for the podocyte. Patients

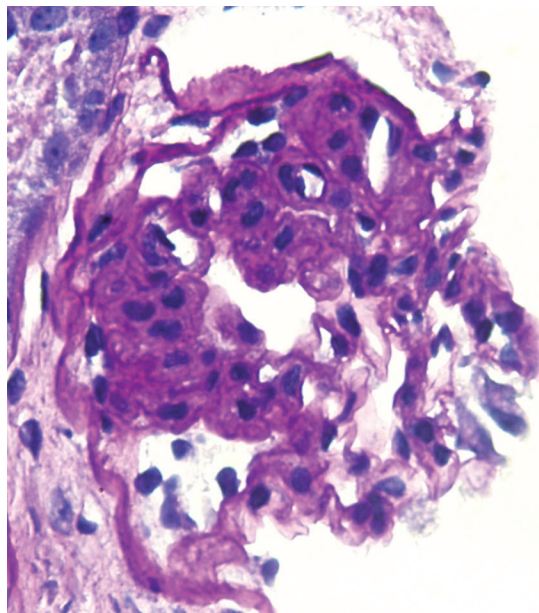


FIG. 3.20 Focal segmental glomerulosclerosis, genetic, due to an *ACTN4* mutation. There is segmental sclerosis, not otherwise specified type, with a mild increase in mesangial matrix and cells, with no specific hints that the underlying etiology is *ACTN4* mutation (periodic acid-Schiff, $\times 400$).

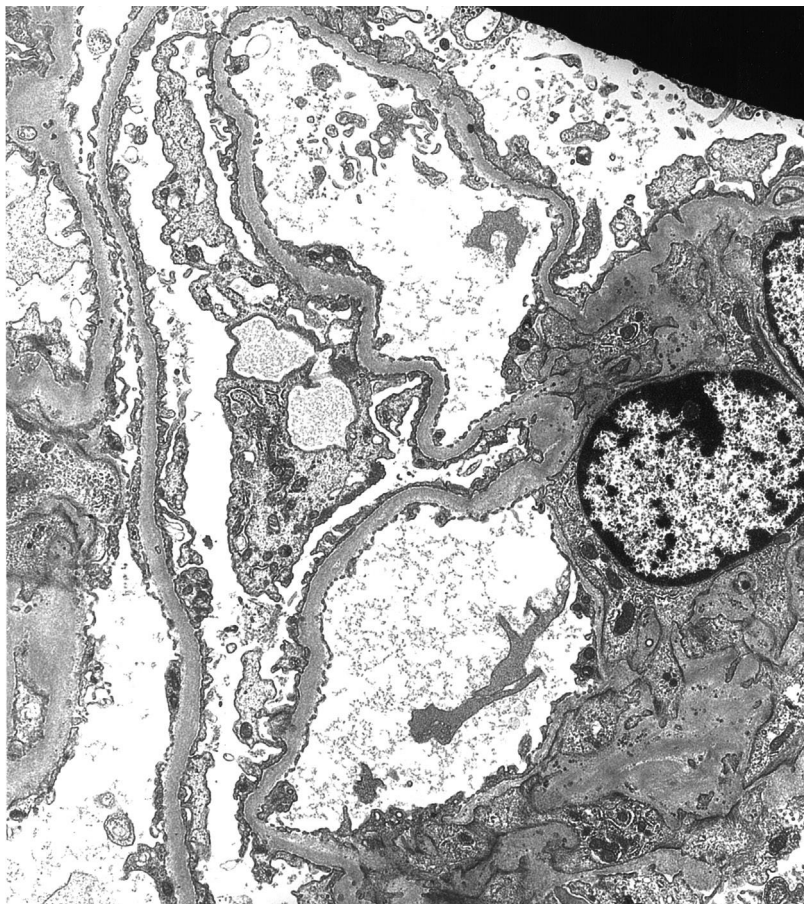


FIG. 3.21 Focal segmental glomerulosclerosis, genetic, due to *ACTN4* mutation. By electron microscopy, there is extensive foot process effacement even in open capillary loops, with occasional vacuoles in podocytes. There are no specific podocyte abnormalities detectable in this case to indicate the underlying mutation causing the FSGS lesions seen in [FIG. 3.20](#) (transmission electron microscopy, $\times 200$).

with *ACTN4* mutation progress to end stage by age 30, with rare recurrence of nephrotic syndrome in the transplant, perhaps related to as-yet-undefined immune reactions to the normal, nonmutated transplant kidney. Transient receptor potential cation channel-6 (TRPC-6) is a channel molecule expressed in the podocyte, and when mutated, a gain-of-function altered calcium flux occurs. FSGS develops in adulthood with variable penetrance. Mutation in inverted formin (*INF2*) is a relatively common cause of autosomal dominant FSGS, and patients present in teenage years or as adults. Podocin, another podocyte-specific gene (*NPHS2*), is mutated in autosomal recessive FSGS that has an early onset in childhood with rapid progression to end-stage kidney disease with frequent steroid resistance. Podocin is an integral stomatin protein family member and interacts with the CD2AP–nephrin complex, indicating that podocin could serve in the structural organization of the slit diaphragm. In contrast to the steroid resistance of the aforementioned, some patients with *PLCE1* mutations may respond to steroids. Acquired disruption of some of these complexly interacting podocyte molecules has been demonstrated in experimental models and in human proteinuric diseases. Genetic variants of apolipoprotein L1 (*APOL1*; G1, G2 variants vs. G0 with no increased risk) that are protective against trypanosomal disease have been linked to increased FSGS in patients of black African ethnicity. Mechanisms for renal disease susceptibility are postulated to involve increased susceptibility of the podocytes to additional second hits in patients homozygous or compound heterozygous for the risk alleles (see “*APOL1*-Associated Nephropathies,” Chapter 6). Thus it is possible that novel molecular and immunostaining techniques to detect abnormalities in these genes and the proteins they encode will become of diagnostic and prognostic utility. For example, some patients with mutations of the *COQ* genes respond to treatment with CoQ10. Mutations

in collagen IV genes, of alpha 3, 4, or 5 chains, causal in autosomal and X-linked forms of Alport, have been found in families with FSGS lesions and proteinuria. Nevertheless, EM showed thin or otherwise abnormal GBM in most, and this may thus represent an unusual part of the spectrum of Alport with FSGS lesions as a major manifestation. In most cases, there currently are no specific morphologic findings recognized to distinguish the FSGS cases caused by genetic mutations from other types of FSGS (see Figs. 3.20–3.21), with the exception of, for example, some features suggestive of CNE, GBM abnormalities suggestive of Alport/*COL4* mutations, and mitochondrial abnormalities in patients with a mutation in mtDNA-A3243G (causing mitochondrial myopathy, encephalopathy, lactic acidosis, stroke-like episodes, MELAS [mitochondrial encephalopathy, lactic acidosis, and stroke-like episodes], and FSGS).

Key Diagnostic Features of Focal Segmental Glomerulosclerosis

- Extensive foot process effacement
- Absence of immune complexes
- Diagnostic segmental lesions

Note: Segmental lesions vary and define the subtype of focal segmental glomerulosclerosis.

Differential Diagnosis of Minimal Change Disease Versus Focal Segmental Glomerulosclerosis

- Global glomerulo sclerosis may be found normally or in any condition and does not differentiate between MCD and FSGS.
- Extent of foot process effacement does not distinguish between primary FSGS and minimal change disease: Less than 50% effacement indicates the process is not likely either untreated MCD or untreated primary FSGS.
- Even in the absence of diagnostic segmental lesions (see earlier), unsampled FSGS may be considered in biopsies with a small sample size.
- Surrogate markers of unsampled FSGS include marked glomerulomegaly and/or interstitial fibrosis in young patients.

FSGS, Focal segmental glomerulosclerosis; MCD, minimal change disease.

Differential Diagnosis of Primary Versus Secondary Focal Segmental Glomerulosclerosis Lesions

- Subtotal (i.e., <50%) foot process effacement strongly favors secondary FSGS.
- Extensive foot process effacement may, however, occasionally occur even in secondary FSGS.
- Key differential features:
 - Arterionephrosclerosis: extensive vascular sclerosis, increased global glomerulosclerosis in solidified pattern, periglomerular fibrosis around nonsclerotic glomeruli, and increased lamina rara interna.
 - Chronic pyelonephritis/reflux nephropathy: sharply delineated, geographic pattern of scarring and thyroidization of tubules, periglomerular fibrosis, and occasionally increased lamina rara interna and subtotal foot process effacement.
- Secondary collapsing glomerulopathy causes:
 - HIVAN; numerous reticular aggregates suggest HIVAN (or possibly lupus nephritis or SARS-CoV-2–associated collapsing glomerulopathy, COVAN).
 - Examples of other secondary causes of collapsing lesions, usually with less extensive foot process effacement: pamidronate toxicity, interferon treatment, severe ischemia (such as that seen with cyclosporin, cocaine), anabolic steroids, SLE, parvovirus. Clinical correlation is essential.

FSGS, Focal segmental glomerulosclerosis; HIVAN, HIV-associated nephropathy; SARS-CoV-2, severe acute respiratory syndrome coronavirus 2; SLE, systemic lupus erythematosus.

Selected Reading

GENERAL

- Braden GL, Mulhern JG, O'Shea MH, et al. Changing incidence of glomerular diseases in adults. *Am J Kidney Dis.* 2000;35:878–883.
- Corwin HL, Schwartz MM, Lewis EJ. The importance of sample size in the interpretation of the renal biopsy. *Am J Nephrol.* 1988;8:85–89.
- D'Agati V. The many masks of focal segmental glomerulosclerosis. *Kidney Int.* 1994;46:1223–1241.
- D'Agati VD, Fogo AB, Bruijn JA, et al. Pathologic classification of focal segmental glomerulosclerosis: A working proposal. *Am J Kidney Dis.* 2004;43:368–382.
- D'Agati VD, Kaskel FJ, Falk RJ. Focal segmental glomerulosclerosis. *N Engl J Med.* 2011;365:2398–2411.
- Deegens JK, Dijkman HB, Borm GF, et al. Podocyte foot process effacement as a diagnostic tool in focal segmental glomerulosclerosis. *Kidney Int.* 2008;74:1568–1576.
- Fatima H, Moeller MJ, Smeets B, et al. Parietal epithelial cell activation marker in early recurrence of FSGS in the transplant. *Clin J Am Soc Nephrol.* 2012;7:1852–1858.
- Fogo AB. Causes and pathogenesis of focal segmental glomerulosclerosis. *Nat Rev Nephrol.* 2015;11:76–87.
- Fogo A, Hawkins EP, Berry PL, et al. Glomerular hypertrophy in minimal change disease predicts subsequent progression to focal glomerular sclerosis. *Kidney Int.* 1990;38:115–123.
- Garin EH, Mu W, Arthur JM, et al. Urinary CD80 is elevated in minimal change disease but not in focal segmental glomerulosclerosis. *Kidney Int.* 2010;78:296–302.
- Gulati S, Sharma AP, Sharma RK, et al. Changing trends of histopathology in childhood nephrotic syndrome. *Am J Kidney Dis.* 1999;3:646–650.
- Haas M, Spargo B, Coventry S. Increasing incidence of focal-segmental glomerulosclerosis among adult nephropathies: A 20-year renal biopsy study. *Am J Kidney Dis.* 1995;26:740–750.
- Hogg R, Middleton J, Vehaskari VM. Focal segmental glomerulosclerosis—epidemiology aspects in children and adults. *Pediatr Nephrol.* 2007;22:183–186.
- Ijpeelaar DH, Farris AB, Goemaere N, et al. Fidelity and evolution of recurrent FSGS in renal allografts. *J Am Soc Nephrol.* 2008;19:2219–2224.
- Smeets B, Stucker F, Wetzels J, et al. Detection of activated parietal epithelial cells on the glomerular tuft distinguishes early focal segmental glomerulosclerosis from minimal change disease. *Am J Pathol.* 2014;184:3239–3248.
- Smith SM, Hoy WE, Cobb L. Low incidence of glomerulosclerosis in normal kidneys. *Arch Pathol Lab Med.* 1989;113:1253–1256.
- Rossini M, Fogo A. Interpreting segmental glomerular sclerosis. *Curr Diagn Pathol.* 2004;10:1–10.

GENETICS

- Boute N, Gribouval O, Roselli S, et al. NPHS2, encoding the glomerular protein podocin, is mutated in autosomal recessive steroid-resistant nephrotic syndrome. *Nat Genet.* 2000;24:349–354.
- Brown EJ, Schlöndorff JS, Becker DJ, et al. Mutations in the formin gene INF2 cause focal segmental glomerulosclerosis. *Nat Genet.* 2010;42:72–76.
- Genovese G, Friedman DJ, Ross MD, et al. Association of trypanolytic ApoL1 variants with kidney disease in African Americans. *Science.* 2010;329:841–845.
- Hildebrandt F, Heeringa SF. Specific podocin mutations determine age of onset of nephrotic syndrome all the way into adult life. *Kidney Int.* 2009;75:669–771.
- Kaplan JM, Kim SH, North KN, et al. Mutations in ACTN4, encoding alpha-actinin-4, cause familial focal segmental glomerulosclerosis. *Nat Genet.* 2000;24:251–256.
- Karle SM, Uetz B, Ronner V, et al. Novel mutations in NPHS2 detected in both familial and sporadic steroid-resistant nephrotic syndrome. *J Am Soc Nephrol.* 2002;13:388–393.
- Lovric S, Ashraf S, Tan W, Hildebrandt F. Genetic testing in steroid-resistant nephrotic syndrome: When and how? *Nephrol Dial Transplant.* 2016;31:1802–1813.
- Ruf RG, Lichtenberger A, Karle SM, et al. Arbeitsgemeinschaft für Pädiatrische Nephrologie Study Group: Patients with mutations in NPHS2 (podocin) do not respond to standard steroid treatment of nephrotic syndrome. *J Am Soc Nephrol.* 2004;15:722–732.
- Sadowski CE, Lovric S, Ashraf S, et al. A single-gene cause in 29.5% of cases of steroid-resistant nephrotic syndrome. *J Am Soc Nephrol.* 2015;26:1279–1289.
- Winn MP, Conlon PJ, Lynn KL, et al. A mutation in the TRPC6 cation channel causes familial focal segmental glomerulosclerosis. *Science.* 2005;308:1801–1804.

COLLAPSING GLOMERULOPATHY

Collapsing glomerulopathy generally has a poor prognosis, with marked proteinuria, rapid loss of renal function, and virtually no responsiveness to corticosteroids alone. Of note, if detected early, prognosis may be less grim. This lesion occurs in both Caucasians and African Americans, with strong African American preponderance, about 85% in a large US-based series. The incidence of this lesion varies in different geographic regions. In New York, the incidence has increased from 11% of all cases of idiopathic FSGS from 1979 to 1985 to 20% of this group from 1986 to 1989 and to 24% of idiopathic FSGS from 1990 to 1993. In a large renal biopsy practice centered in Chicago, the collapsing variant accounted for only 4.7% of FSGS biopsies.

By light microscopy, there is glomerular tuft collapse (segmental or global) and overlying podocyte hyperplasia and hypertrophy (Fig. 3.22). Collapsing lesions are more often global than segmental (Figs. 3.23–3.24; see also Table 3.1). Segmental lesions may involve any portion of the glomerulus (Fig. 3.25). There are frequent marked protein droplets in the hypertrophied visceral epithelial cells (Fig. 3.26). Adhesions and hyalinosis are uncommon in the early stage of the lesion, as are mesangial hypercellularity and glomerulomegaly. Involvement of even a single glomerulus with this collapsing lesion is proposed to warrant classification as collapsing glomerulopathy, with its attendant poor prognosis (Fig. 3.27). Other types of segmental sclerosis (see Table 3.1) may coexist. Differentiation of cellular or collapsing-type FSGS from usual, NOS FSGS may be difficult in some cases (Fig. 3.28). Vessels do not show specific lesions. Tubules show injury disproportionate to the sclerosis with microcystic change (Fig. 3.29), and there is interstitial inflammation.

IF may show IgM and C3 in sclerotic segments. EM shows the wrinkled, collapsed GBM and overlying visceral epithelial cell hypertrophy/hyperplasia with frequent vacuoles and protein droplets. No

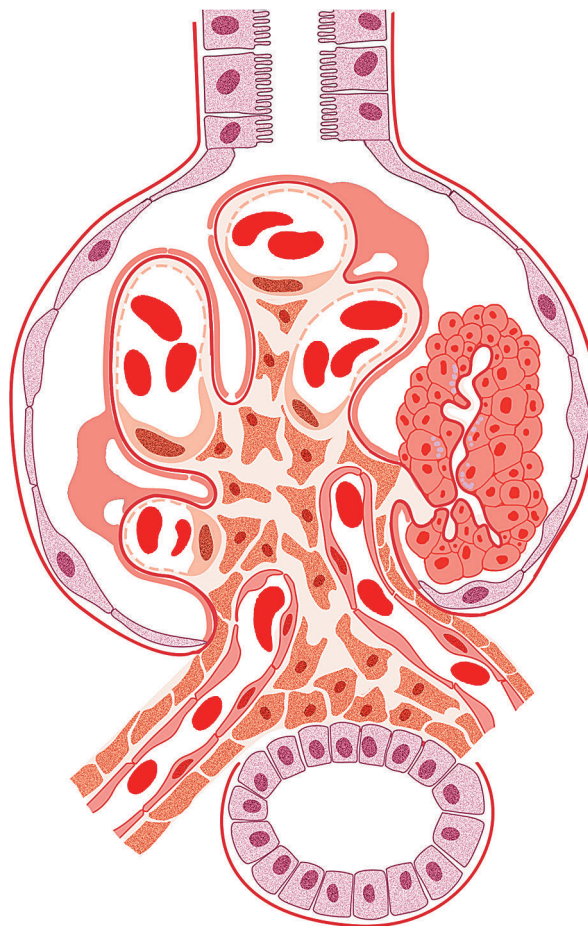


FIG. 3.22 Collapsing glomerulopathy. There is segmental or global collapse of the capillary tuft with overlying visceral epithelial cell hyperplasia, without deposits.

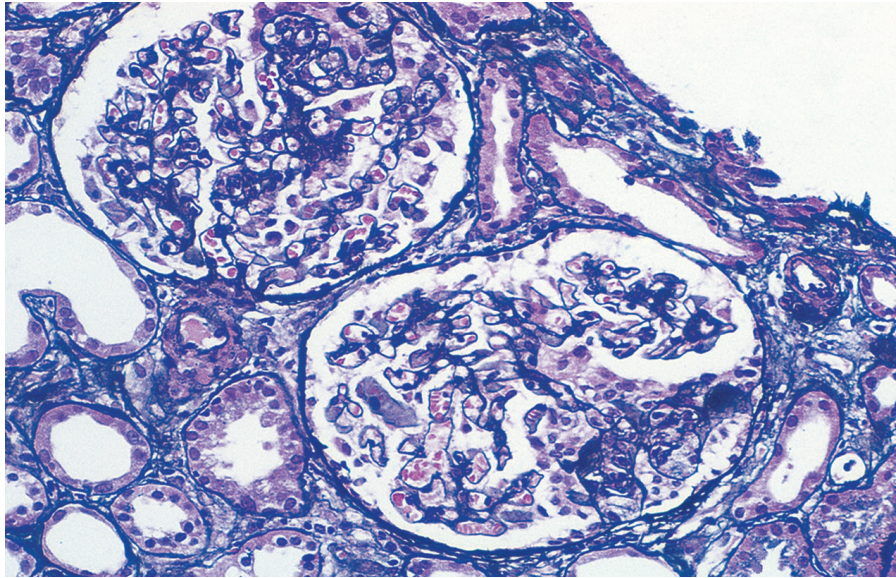


FIG. 3.23 Collapsing glomerulopathy. Collapsing glomerulopathy is characterized by collapse of the glomerular tuft with marked proliferation of overlying visceral epithelial cells, often with prominent protein droplets. The collapse may be global, or more segmental (Jones silver stain, $\times 400$).

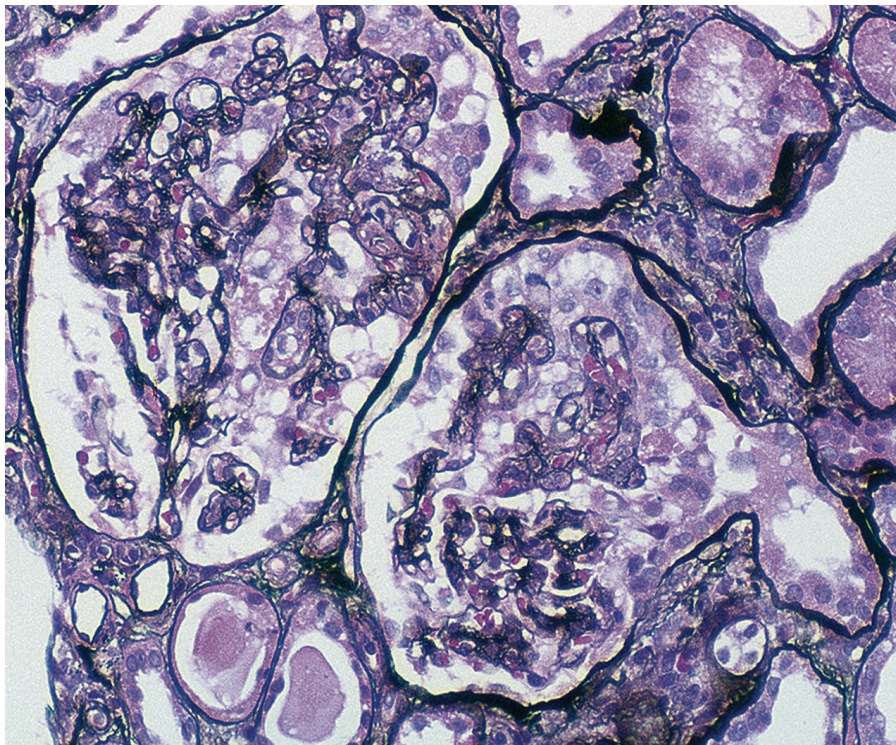


FIG. 3.24 Collapsing glomerulopathy. Extensive collapse with marked visceral epithelial cell hyperplasia in collapsing glomerulopathy (Jones silver stain, $\times 400$).

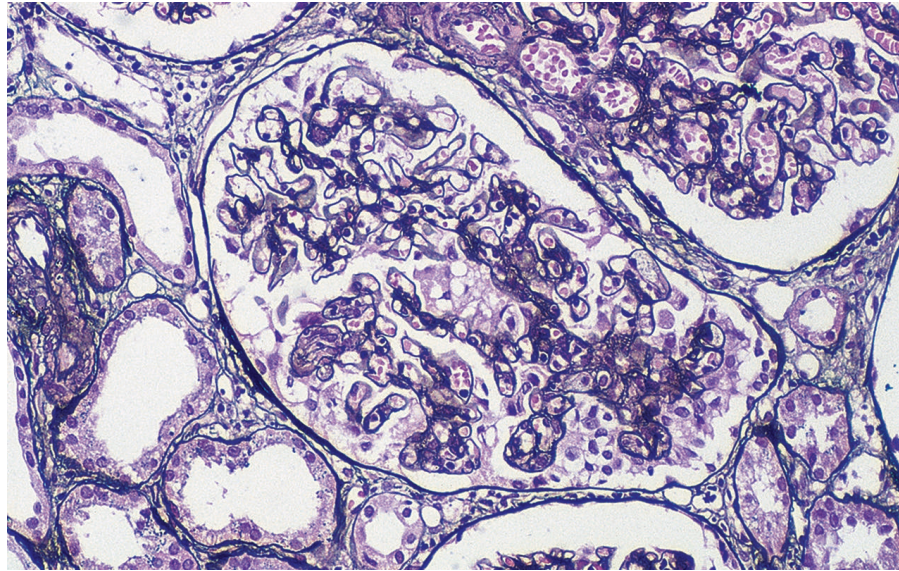


FIG. 3.25 Collapsing glomerulopathy. Occasionally, the collapse may be quite segmental, with the remainder of the glomerular capillary tuft showing no alterations. There is marked segmental collapse with overlying visceral epithelial cell hyperplasia in this case of collapsing glomerulopathy (Jones silver stain, $\times 200$).

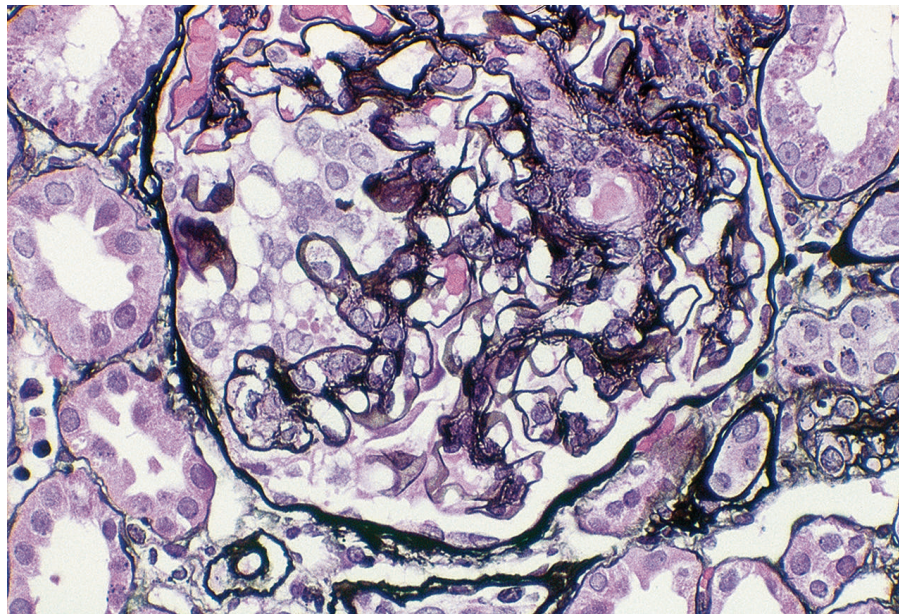


FIG. 3.26 Collapsing glomerulopathy. There is collapse of the glomerular tuft and overlying hyperplasia of the visceral epithelial cells, with prominent protein reabsorption droplets (Jones silver stain, $\times 400$).

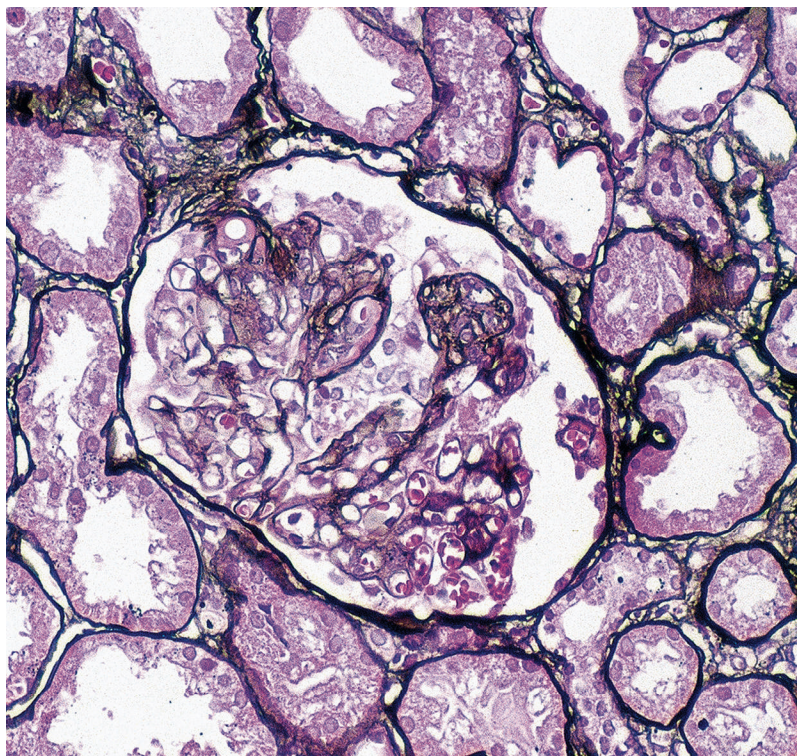


FIG. 3.27 Collapsing glomerulopathy. There are some overlap features between the cellular type of focal segmental glomerulosclerosis and collapsing glomerulopathy, as illustrated here. There is collapse in areas, and segmental endocapillary hypercellularity, with occasional neutrophils and foam cells, with overlying visceral epithelial cell hyperplasia. Nevertheless, the endocapillary hypercellularity is not quite prominent enough to classify as a cellular lesion, and this lesion would best be classified as collapsing glomerulopathy (Jones silver stain, $\times 400$).

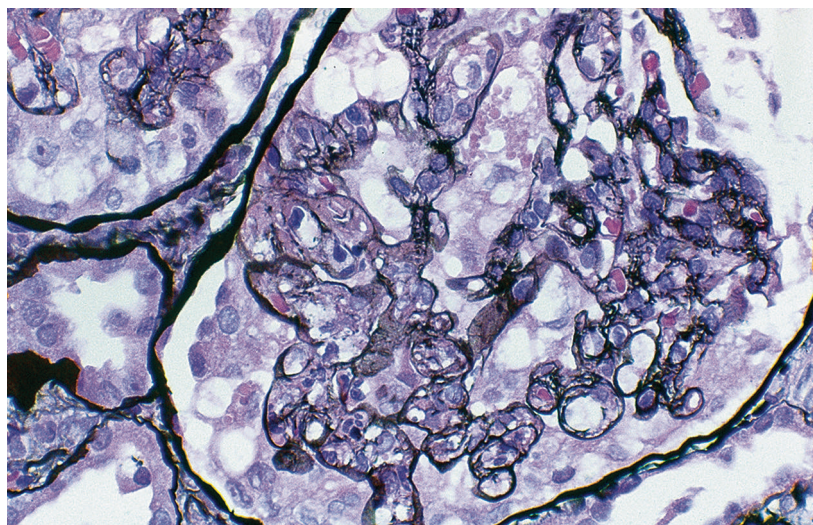


FIG. 3.28 Complex focal segmental glomerulosclerosis (FSGS). This glomerulus shows an early, complex sclerosing lesion with varying features. There is a segmental area of adhesion with hyalinosis (*left*), with mild overlying visceral epithelial cell hypertrophy/hyperplasia. In the adjacent lobule, there is an early cellular lesion with mild endocapillary hypercellularity, but without the typical foam cells of FSGS, cellular variant. There is a small area of collapse at 5 o'clock, and the cellular lesion occupies only a very small portion of the tuft. This is therefore best classified as FSGS, collapsing variant, although it shows some overlapping features with both the cellular and collapsing variants of FSGS (endocapillary hypercellularity and visceral epithelial cell hypertrophy/hyperplasia). This most likely represents an early sclerosing lesion (Jones silver stain, $\times 400$).

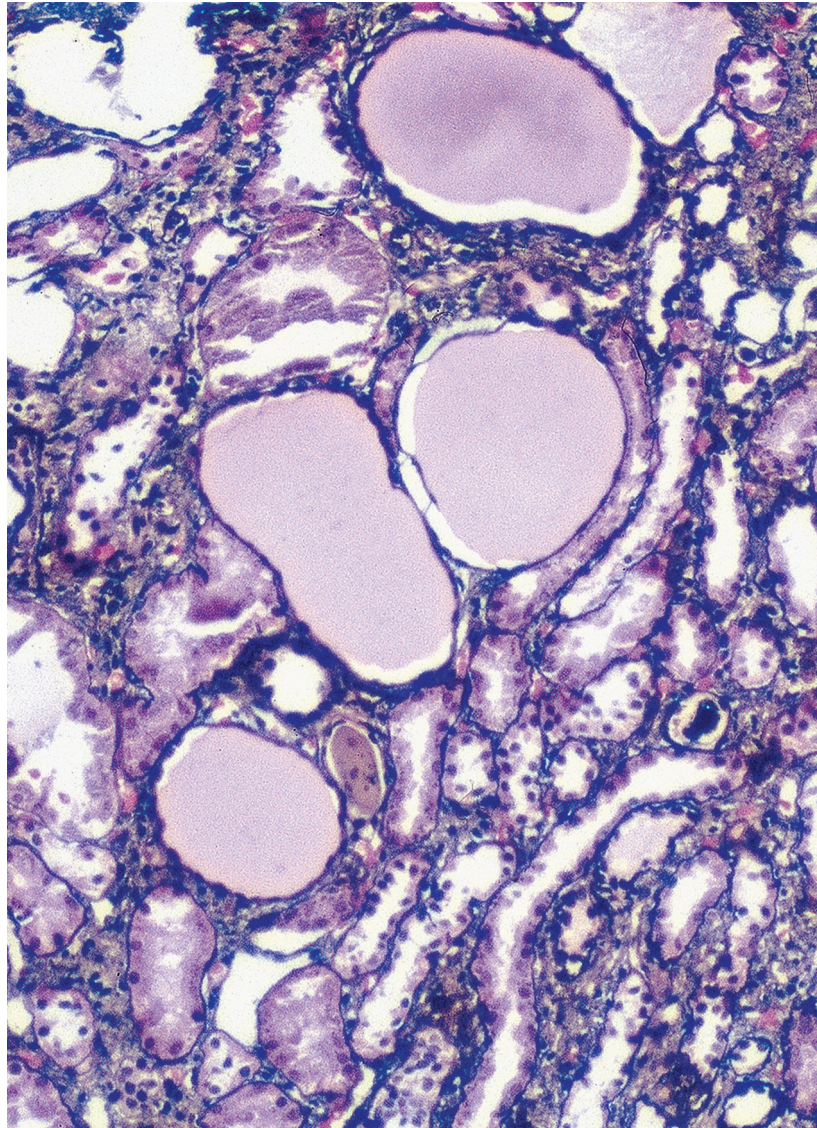


FIG. 3.29 Collapsing glomerulopathy. Collapsing glomerulopathy is often associated with disproportionate tubulointerstitial injury with microcystic change with proteinaceous casts, as shown here (Jones silver stain, $\times 200$).

immune complexes are present (Fig. 3.30). Reticular aggregates are not present in idiopathic collapsing glomerulopathy.

Etiology/Pathogenesis

Mature podocytes do not usually proliferate because of high expression of cyclin-dependent kinase inhibitor p27kip1. In collapsing glomerulopathy and HIVAN, p27kip1 expression is lost in areas of collapse, with proliferation and dedifferentiation, with expression of parietal epithelial cell markers. These observations point to a dysregulated phenotype of these epithelial cells in the pathogenesis of these disorders. Parietal epithelial cells contribute to this hyperplasia and may also migrate along the GBM to replace injured podocytes. The etiology of collapsing glomerulopathy has not yet been defined. Increased risk is associated with presence of homozygous or compound heterozygous states of the apolipoprotein (*APOL1*) risk alleles G1 or G2 rather than G0. The excess incidence of these risk alleles in African Americans is postulated to have evolved because it confers protection against a strain of trypanosomiasis. How these risk alleles of *APOL1* might predispose to podocyte damage and

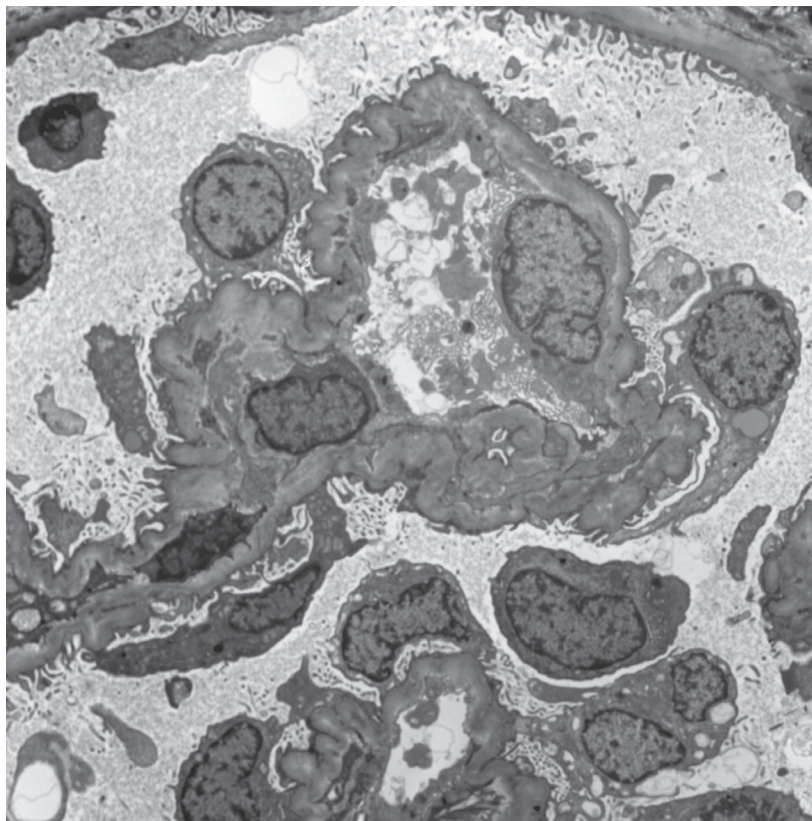


FIG. 3.30 Idiopathic collapsing glomerulopathy. There is extensive corrugation of the glomerular basement membrane with segmental areas of collapse by electron microscopy, without any deposits. Podocytes show extensive foot process effacement, vacuolization, and microvillous transformation (transmission electron microscopy, $\times 5000$).

collapsing glomerulopathy is not determined, with experimental evidence suggesting increased susceptibility of the glomerular epithelial cells to a second hit.

Possible viral agents other than HIV have also been proposed to cause collapsing glomerulopathy. Evidence of parvovirus infection was more frequent in patients with collapsing glomerulopathy compared with controls, usual-type FSGS, or HIVAN, suggesting an association. Possible linkage to cytomegalovirus has been reported. Collapsing glomerulopathy has developed in some patients with SARS-CoV-2, with respiratory manifestations and then marked proteinuria. This lesion appears to particularly occur in SARS-CoV-2 patients with *APOL1* risk allele variants. Treatment with pamidronate or interferon or use of anabolic steroids has been linked to development of collapsing glomerulopathy. Some patients with LN have collapsing lesions, particularly associated with diffuse proliferative lesions of class IV International Society of Nephrology/ Renal Pathology Society (ISN/RPS) LN (see section on “Lupus Nephritis”). Severe ischemia, linked to, for example, severe hypoperfusion, cocaine use, cyclosporine treatment, or thrombotic microangiopathy of varying etiology, has been associated with collapsing lesions. Collapsing glomerular lesions in native kidneys have been noted in a zonal distribution associated with severe vascular injury. Recurrence of collapsing glomerulopathy in the transplant has been reported. De novo collapsing glomerulopathy has also been noted in the transplant, linked to calcineurin inhibitor toxicity.

Selected Reading

- Barisoni L, Kriz W, Mundel P, et al. The dysregulated podocyte phenotype: A novel concept in the pathogenesis of collapsing idiopathic focal segmental glomerulosclerosis and HIV-associated nephropathy. *J Am Soc Nephrol.* 1999;10:51–56.
- Buob D, Decambron M, Gnemmi V, et al. Collapsing glomerulopathy is common in the setting of thrombotic microangiopathy of the native kidney. *Kidney Int.* 2016;90:1321–1331.